

# Mixed Bernstein-Fourier Approximants for Optimal Trajectory Generation with Periodic Behavior

Liraz Mudrik\*, Sean Kragelund†, and Isaac Kaminer‡  
*Naval Postgraduate School, Monterey, CA, 93943*

Efficient trajectory generation is critical for autonomous systems, yet current numerical methods often struggle to handle periodic behaviors effectively, especially when equidistant time nodes are required. This paper introduces a novel mixed Bernstein-Fourier approximation framework tailored explicitly for optimal motion planning. Our proposed methodology leverages the uniform convergence properties of Bernstein polynomials for nonperiodic behaviors while effectively capturing periodic dynamics through the Fourier series. Theoretical results are established, including uniform convergence proofs for approximations of functions, derivatives, and integrals, as well as detailed error bound analyses. We further introduce a regulated least squares approach for determining approximation coefficients, enhancing numerical stability and practical applicability. Within an optimal control context, we establish the feasibility and consistency of approximated solutions to their continuous counterparts. We also extend the covector mapping theorem, providing theoretical guarantees for approximating dual variables crucial in verifying the necessary optimality conditions from Pontryagin’s Maximum Principle. Comprehensive numerical examples illustrate the method’s superior performance, demonstrating substantial improvements in computational efficiency and precision in scenarios with complex periodic constraints and dynamics. Our mixed Bernstein-Fourier

---

\*Postdoctoral fellow, Dept. of Mechanical and Aerospace Engineering. Email: [liraz.mudrik.ctr@nps.edu](mailto:liraz.mudrik.ctr@nps.edu). Member AIAA.

†Research Assistant Professor, Dept. of Mechanical and Aerospace Engineering. Email: [spragel@nps.edu](mailto:spragel@nps.edu).

‡Professor, Mechanical and Aerospace Engineering. Email: [kaminer@nps.edu](mailto:kaminer@nps.edu).

**methodology thus presents a robust, theoretically grounded, and computationally efficient approach for advanced optimal trajectory planning in autonomous systems.**

## **I. Introduction**

Motion planning is critical for autonomous vehicles tasked with executing complex missions in challenging and dynamic environments. Such missions frequently involve navigating around obstacles, efficiently utilizing limited resources, and strictly adhering to operational constraints. Optimal control theory provides an efficient framework for tackling these motion planning problems. Within this theoretical structure, the optimal trajectory is determined by minimizing a carefully chosen objective function, which typically represents cost, energy, or time, subject to a set of constraints. These constraints often include the vehicle's dynamic equations, initial and terminal conditions, and physical limitations such as bounds on speed, acceleration, and control inputs. Due to the complexity inherent in these constraints and objectives, analytical solutions to optimal control problems are extremely rare, necessitating the use of numerical methods.

Direct methods have emerged as the predominant approach for solving optimal control problems numerically. These methods transform the infinite-dimensional continuous-time optimal control problem into a finite-dimensional nonlinear programming (NLP) problem by discretizing the state and control variables over time. This discretization allows the use of readily available numerical solvers to compute approximate solutions efficiently. The theoretical underpinnings that ensure feasibility and consistency of these discretized NLP solutions to the original continuous-time problem have been extensively studied and validated [1, 2]. A wide range of discretization methods have been developed, such as Euler [2], Runge-Kutta [3], Pseudospectral [4], and Bernstein [5]. Each method offers distinct advantages and trade-offs in accuracy, computational complexity, and convergence rates.

Despite their broad adoption and effectiveness, direct methods primarily focus on accurately approximating primal variables—the system states and control inputs—while often neglecting the

dual variables (costates and multipliers) that appear in Pontryagin’s Maximum Principle (PMP) [6]. The PMP provides the necessary conditions for optimality, encompassing both primal and dual variables. The convergence of primal variables alone does not imply the convergence of dual variables, and thus, verifying optimality demands careful consideration of costate convergence. The *covector mapping theorem* bridges this critical gap by explicitly linking solutions from discretized NLP problems back to the PMP conditions. This theorem ensures that the dual variables derived from numerical solutions accurately approximate their continuous-time counterparts. Prior work has successfully established this theorem for various discretization methods, including Runge-Kutta [7], Pseudospectral [8, 9], and Bernstein [10].

Bernstein polynomials possess several beneficial properties for trajectory generation, notably their uniform convergence to the approximated functions and their derivatives. Additionally, Bernstein polynomials feature favorable geometric characteristics, simplifying the computation of critical trajectory constraints like obstacle avoidance and trajectory bounds [11, 12]. Bernstein-based methods utilize equispaced discretization, which contrasts sharply with Pseudospectral approaches requiring non-uniform discretization methods, such as Chebyshev nodes or Birkhoff interpolation [13], even when applied to arbitrary grids [14]. Non-uniform discretizations in Pseudospectral methods are primarily adopted to avoid numerical instabilities like the Runge phenomenon, an oscillatory behavior occurring when uniformly spaced nodes are used to interpolate high-order polynomials. In contrast, Bernstein polynomials do not exhibit the Runge phenomenon due to their inherent numerical stability and uniform convergence properties, thus naturally accommodating uniform time discretization. This equispaced discretization is especially valuable in practical scenarios such as optimal observer trajectory generation, where sensors operate at uniform sampling intervals [15–17]. However, Bernstein polynomials typically exhibit slower convergence compared to Pseudospectral methods [4].

The mixed Bernstein-Fourier approximation approach proposed in this paper is particularly beneficial for motion planning problems exhibiting periodic behaviors, such as optimal observer trajectory generation [15–17] and low-thrust orbit transfers [18, 19]. The primary contributions

of this work are as follows. First, we establish the uniform convergence properties for the mixed Bernstein-Fourier basis, including convergence of the approximated functions, their derivatives, integrals, and explicit error bounds. Next, we introduce a regulated least squares (LS) formulation designed to robustly handle cases that may exhibit clear periodicity that is not straightforward to identify, thereby broadening the applicability of our method. We then demonstrate how this mixed approximation method can effectively address optimal motion planning problems, providing accurate and efficient solutions. Specifically, we provide detailed proofs of feasibility and consistency, showing that the solutions obtained from the approximated problems converge to the true solutions of the original continuous-time optimal control problems. These proofs offer theoretical guarantees on the reliability and accuracy of our approximation approach. Finally, we generalize the covector mapping theorem to accommodate the mixed Bernstein-Fourier context, ensuring precise and reliable approximations of dual variables. Preliminary results using this mixed approximation method were initially presented in an earlier conference paper [20]. This work presents comprehensive numerical simulations that validate the theoretical results and illustrate the practical advantages of our proposed methodology.

This paper is organized as follows. The next section presents the necessary mathematical background of Bernstein polynomials and the Fourier series. Sec. III presents the mixed Bernstein-Fourier approximants and proves the uniform convergence of this approximation, its derivative, and its integral. Sec. IV formulates the motion planning problem using optimal control theory and the approximated version of this problem using the mixed Bernstein-Fourier basis functions, including an analysis that proves the feasibility and consistency of the approximated problem. After proving the covector mapping theorem in Sec. V, we present simulation results in Sec. VI to illustrate the performance of the proposed solution in two examples, followed by concluding remarks.

## **II. Mathematical Background**

This section describes the required mathematical background on using Bernstein and Fourier approximants for function approximation. We first present the notation used in this paper. Bold

letters denote vectors:  $\mathbf{x} = [x_1, \dots, x_m]^T$ . The symbol  $C^r$  denotes the space of functions with  $r$  continuous derivatives, and  $C_m^r$  denotes the space of  $m$ -dimensional vector-valued functions in  $C^r$ .  $\|\cdot\| : C_m^r \rightarrow \mathbb{R}$  denotes the Euclidean norm, that is  $\|\mathbf{x}\| = \sqrt{x_1^2 + \dots + x_m^2}$ . The modulus of continuity is defined for any function  $\mathbf{f} : [0, t_f] \rightarrow \mathbb{R}^{m_f}$  as

$$W_{\mathbf{f}}(\delta) = \max_{|t_1 - t_2| \leq \delta} \|\mathbf{f}(t_1) - \mathbf{f}(t_2)\|, \quad \forall t_1, t_2 \in [0, t_f] \quad (1)$$

where  $m_f$  is the dimension of the function vector  $\mathbf{f}(\cdot)$ . If  $\mathbf{f} \in C_{m_f}^0$  on  $[0, t_f]$ , then  $\lim_{\delta \rightarrow 0} W_{\mathbf{f}}(\delta) = 0$ .

### A. Bernstein Approximation

The Bernstein basis polynomials of order  $n$  are defined as

$$b_{k,n}(t) = \binom{n}{k} \frac{t^k (t_f - t)^{n-k}}{t_f^n}, \quad \forall t \in [0, t_f] \quad (2)$$

where

$$\binom{n}{k} = \frac{n!}{k!(n-k)!}. \quad (3)$$

We denote equidistant time nodes  $t_k = \frac{k}{n}t_f$ ,  $k = 0, \dots, n$ , where  $t_f > 0$  is given. We then use these basis functions to introduce the  $n^{\text{th}}$  approximation of a function

$$\mathbf{f}(t) \approx \mathbf{f}_n(t) = \sum_{k=0}^n \bar{\mathbf{f}}_{k,n} b_{k,n}(t), \quad t \in [0, t_f] \quad (4)$$

where  $\bar{\mathbf{f}}_{k,n} \in \mathbb{R}^{m_f}$ ,  $k = 0, \dots, n$ , are the Bernstein coefficients, satisfying  $\bar{\mathbf{f}}_{k,n} = \mathbf{f}(t_k)$  for all  $k = 0, \dots, n$ . Note that the first and last coefficients of a Bernstein polynomial are its boundary points, that is,  $\mathbf{f}(0) = \bar{\mathbf{f}}_{0,n}$  and  $\mathbf{f}(t_f) = \bar{\mathbf{f}}_{n,n}$ .

We can also approximate the time derivative of the function using the following differentiation

property

$$\dot{\mathbf{f}}_n(t) = \sum_{k=0}^{n-1} \frac{n}{t_f} (\bar{\mathbf{f}}_{k+1,n} - \bar{\mathbf{f}}_{k,n}) b_{k,n-1}(t) = \frac{1}{t_f} \sum_{k=0}^{n-1} \sum_{i=0}^n \bar{\mathbf{f}}_{i,n} \mathbf{D}_{i,k} b_{k,n-1}(t) \quad (5)$$

where  $\mathbf{D}_{i,k}$  is the  $(i, k)$  element of the differentiation matrix, satisfying

$$\mathbf{D} = \begin{bmatrix} -n & 0 & \cdots & 0 \\ n & -n & \cdots & 0 \\ \vdots & \ddots & \ddots & \\ 0 & \cdots & n & -n \\ 0 & \cdots & 0 & n \end{bmatrix} \in \mathbb{R}^{(n+1) \times n}. \quad (6)$$

**Lemma II.1** (Uniform Convergence, see [21]). *Let  $\mathbf{f} \in C_{m_f}^0$  on  $[0, t_f]$ . Its Bernstein approximation, defined in Eq. (4), satisfies for any  $n \in \mathbb{N}$*

$$\|\mathbf{f}(t) - \mathbf{f}_n(t)\| \leq C_0 W_{\mathbf{f}}\left(\frac{1}{\sqrt{n}}\right) \quad (7)$$

where  $C_0$  is a positive constant independent of  $n$  and  $W_{\mathbf{f}}(\cdot)$  is the modulus of continuity of  $\mathbf{f}$  in  $[0, t_f]$ .

If  $\mathbf{f} \in C_{m_f}^1$  on  $[0, t_f]$ , then

$$\|\dot{\mathbf{f}}(t) - \dot{\mathbf{f}}_n(t)\| \leq C_1 W_{\dot{\mathbf{f}}}\left(\frac{1}{\sqrt{n}}\right) \quad (8)$$

where  $C_1$  is a positive constant independent of  $n$  and  $W_{\dot{\mathbf{f}}}(\cdot)$  is the modulus of continuity of  $\dot{\mathbf{f}}$  in  $[0, t_f]$ .

Integrating the approximated state vector is readily computed as

$$\int_0^{t_f} \mathbf{f}_n(t) dt = \frac{t_f}{n+1} \sum_{k=0}^n \bar{\mathbf{f}}_{k,n}. \quad (9)$$

**Lemma II.2** (Uniform Convergence of the Integral, see [5]). *If  $\mathbf{f} \in C_{m_f}^0$  on  $[0, t_f]$ , then*

$$\left\| \int_0^{t_f} \mathbf{f}(t) dt - \frac{t_f}{n+1} \sum_{k=0}^n \bar{\mathbf{f}}_{k,n} \right\| \leq C_I W_{\mathbf{f}} \left( \frac{1}{\sqrt{n}} \right) \quad (10)$$

where  $C_I$  is a positive constant independent of  $n$ .

## B. Fourier Series

A function  $\mathbf{p}(t)$  is generally said to be  $t_f$ -periodic if  $\mathbf{p}(t) = \mathbf{p}(t + t_f)$  for any  $t \in \mathbb{R}$ . In this work, we consider  $t \in [0, t_f]$ , so we say that any function that satisfies  $\mathbf{p}(0) = \mathbf{p}(t_f)$  is periodic on  $[0, t_f]$ .

The Fourier series of such a periodic function  $\mathbf{p}(t) \in C_{m_p}^r$  on  $[0, t_f]$  is constructed as

$$\mathbf{S}_n(t) = \frac{\mathbf{a}_0}{2} + \sum_{k=1}^n \left[ \mathbf{a}_k \cos \left( \frac{2\pi kt}{t_f} \right) + \mathbf{b}_k \sin \left( \frac{2\pi kt}{t_f} \right) \right] \quad (11)$$

whose coefficients satisfy

$$\mathbf{a}_k = \frac{2}{t_f} \int_0^{t_f} \mathbf{p}(t) \cos \left( \frac{2\pi kt}{t_f} \right) dt, \quad \forall k = 0, \dots, n, \quad (12)$$

$$\mathbf{b}_k = \frac{2}{t_f} \int_0^{t_f} \mathbf{p}(t) \sin \left( \frac{2\pi kt}{t_f} \right) dt, \quad \forall k = 1, \dots, n. \quad (13)$$

**Lemma II.3.** (Uniform Convergence of Periodic Function, see Sec. I.3 in [22]) *If  $\mathbf{p}(t) \in C_{m_p}^r$  is periodic on  $[0, t_f]$ , where  $r \in \mathbb{Z}^+$ , then its Fourier approximation, defined in Eq. (11), satisfies for any  $n \in \mathbb{N}$*

$$\|\mathbf{p}(t) - \mathbf{S}_n(t)\| \leq \frac{A_0 \log n}{n^r} W_{\mathbf{p}} \left( \frac{2\pi}{n} \right) \quad (14)$$

where  $A_0$  is a positive constant independent of  $n$  and  $W_{\mathbf{p}}(\cdot)$  is the modulus of continuity of  $\mathbf{p}$  in  $[0, t_f]$ .

*If  $\dot{\mathbf{p}}(t)$  is also periodic on  $[0, t_f]$  and  $r \geq 1$ , then*

$$\|\dot{\mathbf{p}}(t) - \dot{\mathbf{S}}_n(t)\| \leq \frac{A_1 \log n}{n^{r-1}} W_{\dot{\mathbf{p}}} \left( \frac{2\pi}{n} \right) \quad (15)$$

where  $A_1$  is a positive constant independent of  $n$  and  $W_{\mathbf{p}}(\cdot)$  is the modulus of continuity of  $\mathbf{p}$  in  $[0, t_f]$ .

**Remark 1.** The integral of periodic functions over their period,  $\mathbf{P}(t) \triangleq \int_t^{t+t_f} \mathbf{p}(t') dt'$ , are constant for any  $t \in \mathbb{R}$ :

$$\frac{d\mathbf{P}(t)}{dt} = \mathbf{p}(t + t_f) - \mathbf{p}(t) = \mathbf{0}. \quad (16)$$

Therefore, the integral of the Fourier series is an exact approximation of  $\mathbf{P}(0)$ :

$$\int_0^{t_f} \mathbf{S}_n(t) dt = \frac{\mathbf{a}_0 t_f}{2} = \frac{t_f}{2} \frac{2}{t_f} \int_0^{t_f} \mathbf{p}(t) dt = \mathbf{P}(0). \quad (17)$$

### III. Mixed Bernstein-Fourier Basis for Approximation Theory

This section shows how the mixed Bernstein-Fourier basis functions can be used to approximate continuous functions.

#### A. Foundations of the Mixed Bernstein-Fourier Basis

We first note that for any periodic function,  $\mathbf{p}(t)$ , we can use the following relation, which trivially holds for any  $t \in [0, t_f]$ :

$$\mathbf{f}(t) = (\mathbf{f}(t) - \mathbf{p}(t)) + \mathbf{p}(t) = \mathbf{g}(t) + \mathbf{p}(t) \quad (18)$$

where  $\mathbf{g}(t) \triangleq \mathbf{f}(t) - \mathbf{p}(t)$ . This also implies that  $m_{\mathbf{f}} = m_{\mathbf{p}} = m_{\mathbf{g}}$ .

**Remark 2.** When the function  $\mathbf{f}(t)$  does not exhibit periodic behavior, e.g., it is a straight line, the periodic component can be chosen as the zero function  $\mathbf{p}(t) \equiv \mathbf{0}$ . In this case, the mixed Bernstein-Fourier approximation reduces to the classical Bernstein-only approximation.

Then, we can present the mixed approximation using both Bernstein polynomials and Fourier

series

$$\mathbf{T}_n(t) = \sum_{k=0}^{n_g} \bar{\mathbf{g}}_k b_{k,n_g}(t) + \frac{\mathbf{a}_0}{2} + \sum_{k=1}^{n_p} \left[ \mathbf{a}_k \cos\left(\frac{2\pi kt}{t_f}\right) + \mathbf{b}_k \sin\left(\frac{2\pi kt}{t_f}\right) \right] \quad (19)$$

where  $n_g \in \mathbb{N}$  and  $n_p \in \mathbb{N}$  are the orders of approximation of the nonperiodic and periodic parts, respectively,  $n \triangleq \min(n_g, n_p)$ , and the coefficients satisfy

$$\bar{\mathbf{g}}_k = \mathbf{f}\left(\frac{k}{n_g}t_f\right) - \mathbf{p}\left(\frac{k}{n_g}t_f\right), \quad \forall k = 0, \dots, n_g, \quad (20)$$

$$\mathbf{a}_k = \frac{2}{t_f} \int_0^{t_f} \mathbf{p}(t) \cos\left(\frac{2\pi kt}{t_f}\right) dt, \quad \forall k = 0, \dots, n_p, \quad (21)$$

$$\mathbf{b}_k = \frac{2}{t_f} \int_0^{t_f} \mathbf{p}(t) \sin\left(\frac{2\pi kt}{t_f}\right) dt, \quad \forall k = 1, \dots, n_p. \quad (22)$$

**Remark 3.** *At the end points, the mixed approximation satisfies*

$$\mathbf{T}_n(0) = \bar{\mathbf{g}}_0 + \frac{\mathbf{a}_0}{2} + \sum_{k=1}^{n_p} \mathbf{a}_k, \quad (23)$$

$$\mathbf{T}_n(t_f) = \bar{\mathbf{g}}_{n_g} + \frac{\mathbf{a}_0}{2} + \sum_{k=1}^{n_p} \mathbf{a}_k. \quad (24)$$

## B. Mathematical Properties and Convergence

Define the approximation error upper bound of the approximated function  $\mathbf{f}$  and its derivative to be:

$$\delta_{\mathbf{f}}^n \triangleq C_0 W_{\mathbf{g}}\left(\frac{1}{\sqrt{n_g}}\right) + \frac{A_0 \log n_p}{n_p^r} W_{\mathbf{p}}\left(\frac{2\pi}{n_p}\right), \quad (25)$$

$$\delta_{\dot{\mathbf{f}}}^n \triangleq C_1 W_{\dot{\mathbf{g}}}\left(\frac{1}{\sqrt{n_g}}\right) + \frac{A_1 \log n_p}{n_p^{r-1}} W_{\dot{\mathbf{p}}}\left(\frac{2\pi}{n_p}\right). \quad (26)$$

**Theorem III.1.** *Let  $\mathbf{f}(t) \in C_{m_f}^0$  on  $[0, t_f]$ , and its approximation be calculated according to Eq. (19).*

Then, there exists a periodic function  $\mathbf{p} \in C_{m_f}^r, r \geq 0$  on  $[0, t_f]$  such that

$$\|\mathbf{f}(t) - \mathbf{T}_n(t)\| \leq \delta_f^n \quad (27)$$

for any  $n_g, n_p \in \mathbb{N}$ .

*Proof.* The existence of  $\mathbf{p}(t)$  is guaranteed as the zero function, i.e.,  $\mathbf{p}(t) \equiv \mathbf{0}$ , satisfies the periodicity property. Consider:

$$\begin{aligned} \|\mathbf{f}(t) - \mathbf{T}_n(t)\| &= \|\mathbf{g}(t) + \mathbf{p}(t) - \mathbf{T}_n(t)\| \\ &= \left\| \mathbf{g}(t) - \sum_{k=0}^{n_g} \bar{\mathbf{g}}_k b_k(t) + \mathbf{p}(t) - \frac{\mathbf{a}_0}{2} - \sum_{k=1}^{n_p} \left[ \mathbf{a}_k \cos\left(\frac{2\pi kt}{t_f}\right) + \mathbf{b}_k \sin\left(\frac{2\pi kt}{t_f}\right) \right] \right\| \\ &\leq \left\| \mathbf{g}(t) - \sum_{k=0}^{n_g} \bar{\mathbf{g}}_k b_k(t) \right\| + \left\| \mathbf{p}(t) - \frac{\mathbf{a}_0}{2} - \sum_{k=1}^{n_p} \left[ \mathbf{a}_k \cos\left(\frac{2\pi kt}{t_f}\right) + \mathbf{b}_k \sin\left(\frac{2\pi kt}{t_f}\right) \right] \right\| \end{aligned} \quad (28)$$

where the first equality holds due to the relation in Eqs. (18) and (19) and the inequality holds by the triangle inequality. Using Lemma II.1, we get that

$$\left\| \mathbf{g}(t) - \sum_{k=0}^{n_g} \bar{\mathbf{g}}_k b_k(t) \right\| \leq C_0 W_g \left( \frac{1}{\sqrt{n_g}} \right) \quad (29)$$

where  $\bar{\mathbf{g}}_k$  are calculated according to (20). Similarly, using Lemma II.3, we get that

$$\left\| \mathbf{p}(t) - \frac{\mathbf{a}_0}{2} - \sum_{k=1}^{n_p} \left[ \mathbf{a}_k \cos\left(\frac{2\pi kt}{t_f}\right) + \mathbf{b}_k \sin\left(\frac{2\pi kt}{t_f}\right) \right] \right\| \leq \frac{A_0 \log n_p}{n_p^r} W_p \left( \frac{2\pi}{n_p} \right) \quad (30)$$

where  $\mathbf{a}_k$  and  $\mathbf{b}_k$  are calculated according to (21) and (22), respectively, and the result follows.  $\square$

The following example shows the advantages of using the mixed approximation when there is a known periodic component.

**Example III.1.** Consider  $f(t) = t + \sin(2\pi t - 0.5)$  on  $[0, 1]$ . In this case, we readily identify the periodic part as  $p(t) = \sin(2\pi t - 0.5)$  and the non-periodic part as  $g(t) = t$ . We approximate  $f(t)$

with a mixture of first order Bernstein and Fourier approximants,

$$T_1(t) = g_1 t + a_1 \cos(2\pi t) + b_1 \sin(2\pi t) \quad (31)$$

where  $g_1 = 1$ ,  $a_1 = -\sin 0.5$ , and  $b_1 = \cos 0.5$ . Note that this approximation has a total of five coefficients, but  $g_0 = a_0 = 0$ . This approximation is exact, i.e.,  $T_1(t) = f(t)$  for any  $t \in [0, 1]$ .

Fig. 1 illustrates the benefit of using mixed Bernstein-Fourier basis functions to approximate  $f(t)$ , rather than using Bernstein polynomials alone, even for polynomials of order 5, 20, and 100. Adding the Fourier series to the approximant exploits the periodic behavior of the sine function, greatly improving the quality of the approximation. Note that using only a Fourier series approximant in this case does not uniformly converge because  $f(t)$  is not a periodic function.

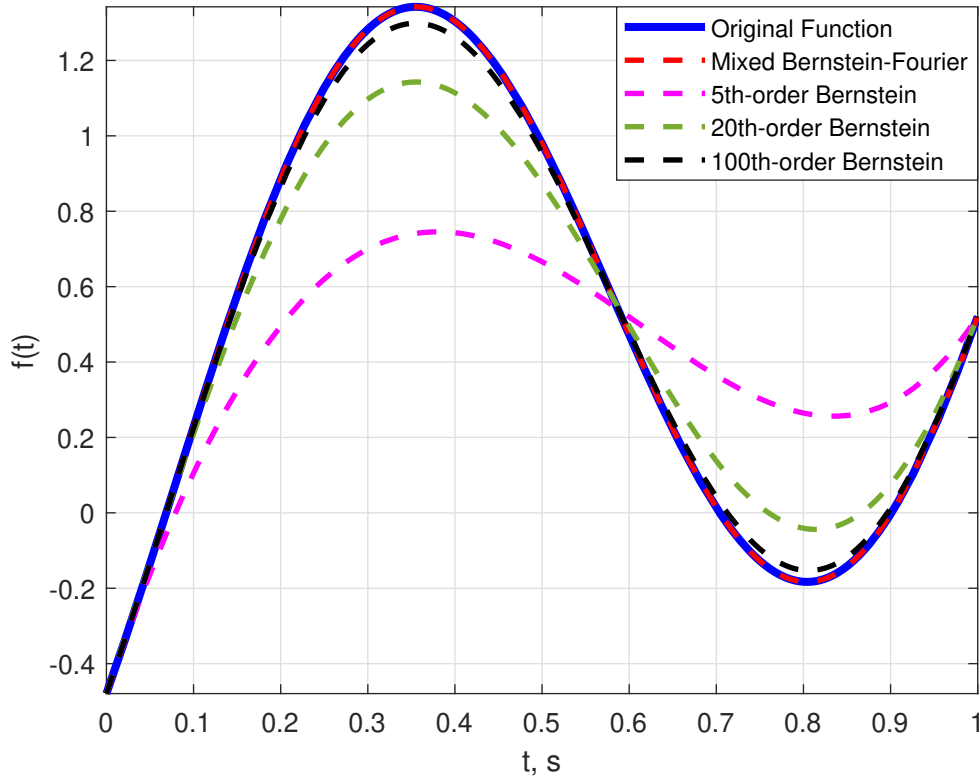


**Figure 1** Approximation of  $f(t) = t + \sin(2\pi t - 0.5)$  (blue line) using mixed Bernstein-Fourier approximants (dashed red line), 5<sup>th</sup>-order Bernstein (dashed magenta line), 20<sup>th</sup>-order Bernstein (dashed green line), and 100<sup>th</sup>-order Bernstein approximation (dashed black line).

The derivative of the mixed approximation is:

$$\dot{\mathbf{T}}_n(t) = \frac{1}{t_f} \sum_{j=0}^{n_g-1} \sum_{k=0}^{n_g} \bar{\mathbf{g}}_k \mathbf{D}_{k,j} b_{j,n-1}(t) + \frac{2\pi}{t_f} \sum_{k=1}^{n_p} k \left[ \mathbf{b}_k \cos\left(\frac{2\pi kt}{t_f}\right) - \mathbf{a}_k \sin\left(\frac{2\pi kt}{t_f}\right) \right]. \quad (32)$$

**Corollary III.1.1.** *Let  $\mathbf{f}(t) \in C_{m_f}^1$  on  $[0, t_f]$ , then for any  $n_g, n_p \in \mathbb{N}$*

$$\|\dot{\mathbf{f}}(t) - \dot{\mathbf{T}}_n(t)\| \leq \delta_{\dot{\mathbf{f}}}^n. \quad (33)$$

We also need to approximate the integral of functions; we use  $n_g + 1$  time steps as done in (9) for the Bernstein-based approximation, yielding the following relation

$$\int_0^{t_f} \mathbf{T}_n(t) dt = \frac{t_f}{n_g + 1} \sum_{k=0}^{n_g} \bar{\mathbf{g}}_k + \frac{\mathbf{a}_0 t_f}{2} = w \sum_{k=0}^{n_g} \left( \bar{\mathbf{g}}_k + \frac{\mathbf{a}_0 t_f}{2w} \right) \quad (34)$$

where  $w = \frac{t_f}{n_g+1}$ .

**Theorem III.2.** *If  $\mathbf{f}(t) \in C_{m_f}^0$  on  $[0, t_f]$ , then*

$$\left\| \int_0^{t_f} \mathbf{f}(t) dt - w \sum_{k=0}^{n_g} \left( \bar{\mathbf{g}}_k + \frac{\mathbf{a}_0 t_f}{2w} \right) \right\| \leq C_I W_{\mathbf{f}} \left( \frac{1}{\sqrt{n}} \right). \quad (35)$$

*Proof.* Using the relations from (18) and (34) and applying the triangle inequality, we get

$$\left\| \int_0^{t_f} \mathbf{f}(t) dt - w \sum_{k=0}^{n_g} \left( \bar{\mathbf{g}}_k + \frac{\mathbf{a}_0 t_f}{2w} \right) \right\| \leq \left\| \int_0^{t_f} \mathbf{g}(t) dt - \frac{t_f}{n_g + 1} \sum_{k=0}^{n_g} \bar{\mathbf{g}}_k \right\| + \left\| \int_0^{t_f} \mathbf{p}(t) dt - \frac{\mathbf{a}_0 t_f}{2} \right\| \quad (36)$$

and the result follows by applying Lemma II.2 and Eq. (17).  $\square$

### C. Approximation Using Regulated Least Squares

Whereas some continuous functions contain obviously periodic components, others may have hidden periodic behavior. Thus, we can formulate a least squares (LS) problem to optimally find the coefficients of a mixed basis that approximates the given function or data points. We now illustrate

this method for the case of a scalar function, but generalization to vector-valued functions is trivial. We use equidistant time nodes  $t_k = \frac{k}{n_t} t_f$  for all  $k = 0, \dots, n_t$ , where  $1/n_t$  is the spacing in time. Consider a given function or data using these time nodes:

$$y = \begin{bmatrix} y_0 & \cdots & y_{n_t} \end{bmatrix}^T \in \mathbb{R}^{n_t+1}. \quad (37)$$

Define the Bernstein-Fourier basis matrix:

$$B = \begin{bmatrix} b_{0,n_g}(t_0) & \cdots & b_{n_g,n_g}(t_0) & \frac{1}{2} & c_1(t_0) & \cdots & c_{n_p}(t_0) & s_1(t_0) & \cdots & s_{n_p}(t_0) \\ b_{0,n_g}(t_1) & \cdots & b_{n_g,n_g}(t_1) & \frac{1}{2} & c_1(t_1) & \cdots & c_{n_p}(t_1) & s_1(t_1) & \cdots & s_{n_p}(t_1) \\ \vdots & & \vdots & \vdots & \vdots & & \vdots & \vdots & & \vdots \\ b_{0,n_g}(t_{n_t}) & \cdots & b_{n_g,n_g}(t_{n_t}) & \frac{1}{2} & c_1(t_{n_t}) & \cdots & c_{n_p}(t_{n_t}) & s_1(t_{n_t}) & \cdots & s_{n_p}(t_{n_t}) \end{bmatrix} \quad (38)$$

where  $B \in \mathbb{R}^{(n_t+1) \times (n_{\text{tot}})}$ ,  $n_{\text{tot}} = n_g + 2n_p + 2$ ,  $c_j(t_k) \triangleq \cos\left(\frac{2\pi j t_k}{t_f}\right)$  and  $s_j(t_k) \triangleq \sin\left(\frac{2\pi j t_k}{t_f}\right)$ , and the decision vector:

$$\mathbf{d} = \begin{bmatrix} \bar{g}_0 & \cdots & \bar{g}_{n_g} & a_0 & \cdots & a_{n_p} & b_1 & \cdots & b_{n_p} \end{bmatrix}^T \in \mathbb{R}^{n_{\text{tot}}}. \quad (39)$$

Thus, we aim to solve the following LS problem [23]:

$$\min_{\mathbf{d}} \|B\mathbf{d} - y\| \quad (40)$$

which has the known solution:

$$\mathbf{d}^* = (B^T B)^{-1} B^T y. \quad (41)$$

The solution exists when the columns of  $B$  are linearly independent; thus, we must ensure that  $n_t \geq n_{\text{tot}} - 1$ . However, even when this condition holds, numerical difficulties exist in the inversion of  $B^T B$ . Therefore, in such cases, we recommend the addition of a Tikhonov regulator to improve

numerical stability. The regulated LS problem is:

$$\min_{\mathbf{d}} \|\mathbf{B}\mathbf{d} - \mathbf{y}\| + \lambda\|\mathbf{d}\| \quad (42)$$

where  $\lambda$  is the regularization parameter. The solution is known to be:

$$\mathbf{d}^* = (\mathbf{B}^T \mathbf{B} + \lambda \mathbf{I})^{-1} \mathbf{B}^T \mathbf{y} \quad (43)$$

where  $\mathbf{I}$  is the identity matrix.

**Example III.2.** *We consider a case of data fitting using the mixed Bernstein-Fourier approximants. Fig. 2 presents data obtained from uniform sampling at a frequency of 100 Hz. While this plot clearly shows oscillations, the functional form of these oscillations is not straightforward. Therefore, we use LS and regulated LS techniques to find coefficients for different approximants, namely for Bernstein-only, Fourier-only, and the proposed mixed basis approximants.*

*The Bernstein-only LS problem is solved by applying the solutions for the LS problem in (41) or the regulated LS problem in (43) to the first  $n_{\mathbf{g}} + 1$  columns of matrix  $\mathbf{B}$  and the first  $n_{\mathbf{g}} + 1$  entries of  $\mathbf{d}$ . Similarly, we can solve the Fourier-only LS problem using the last  $2n_{\mathbf{p}} + 1$  columns of matrix  $\mathbf{B}$  and the last  $2n_{\mathbf{p}} + 1$  entries of  $\mathbf{d}$ . For simplicity of exposition, we set  $n = n_{\mathbf{g}} = n_{\mathbf{p}}$ . Hence, the dimensions for the decision vector for different approximants are*

$$\dim(\mathbf{d}) = \begin{cases} n + 1, & \text{Bernstein - only} \\ 2n + 1, & \text{Fourier - only} \\ 3n + 2, & \text{Mixed Bernstein - Fourier} \end{cases} \quad (44)$$

*Fig. 3 presents the mean of the root mean square (RMS) error with respect to time vs. decision vector dimension for different function approximations. We observe that mixed Bernstein-Fourier approximants have the smallest RMS errors, approximately three times lower than Bernstein-only approximants and ten times smaller than Fourier-only approximants. Moreover, we note that the*

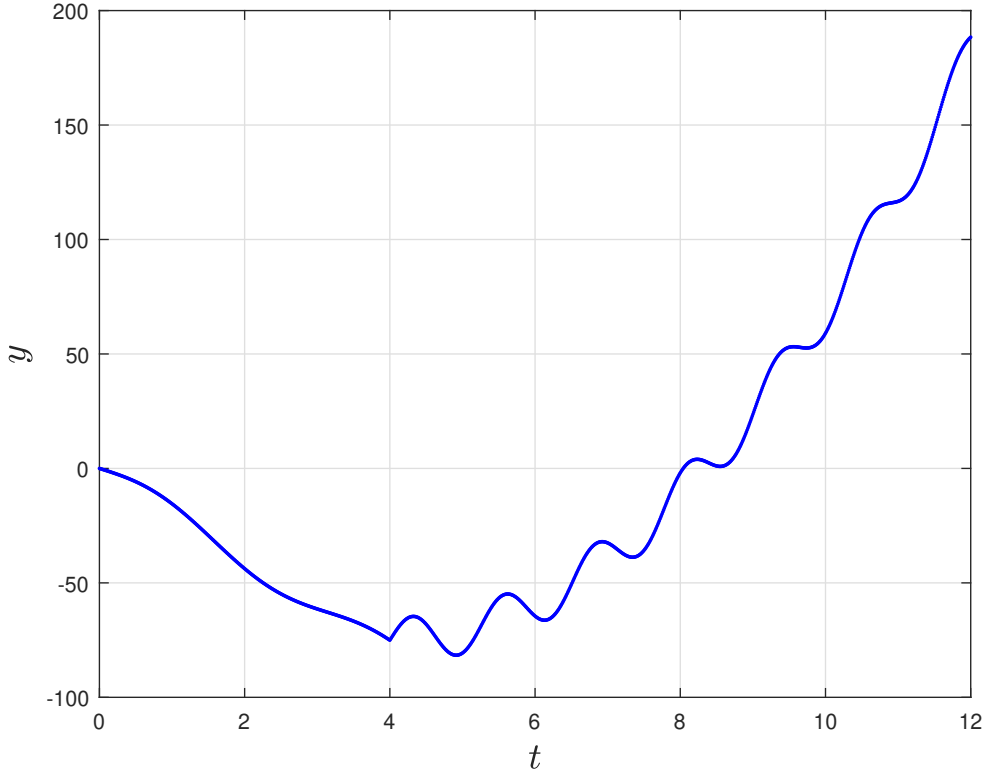


**Figure 2** The data to be approximated.

*regularization term improves the solution's numerical stability, especially for the Bernstein-only case. Even a very small regularization value,  $\lambda = 10^{-14}$  in this case, makes the resulting LS solution more reliable and consistent.*

In the ensuing section, we formulate an approximated version of the optimal motion planning problem using mixed Bernstein-Fourier approximants. The regulated LS technique described above is used to find the Bernstein-Fourier coefficients for a given trajectory, which are needed to provide an initial guess to the NLP optimizer.

#### **IV. Optimal Motion Planning Problem**

This section presents the optimal primal motion planning problem using a normalized time scale, as presented for the Bernstein-only case in [10]. We first generally formulate the problem and then present the approximated problem using the mixed Bernstein-Fourier approximants. We then prove

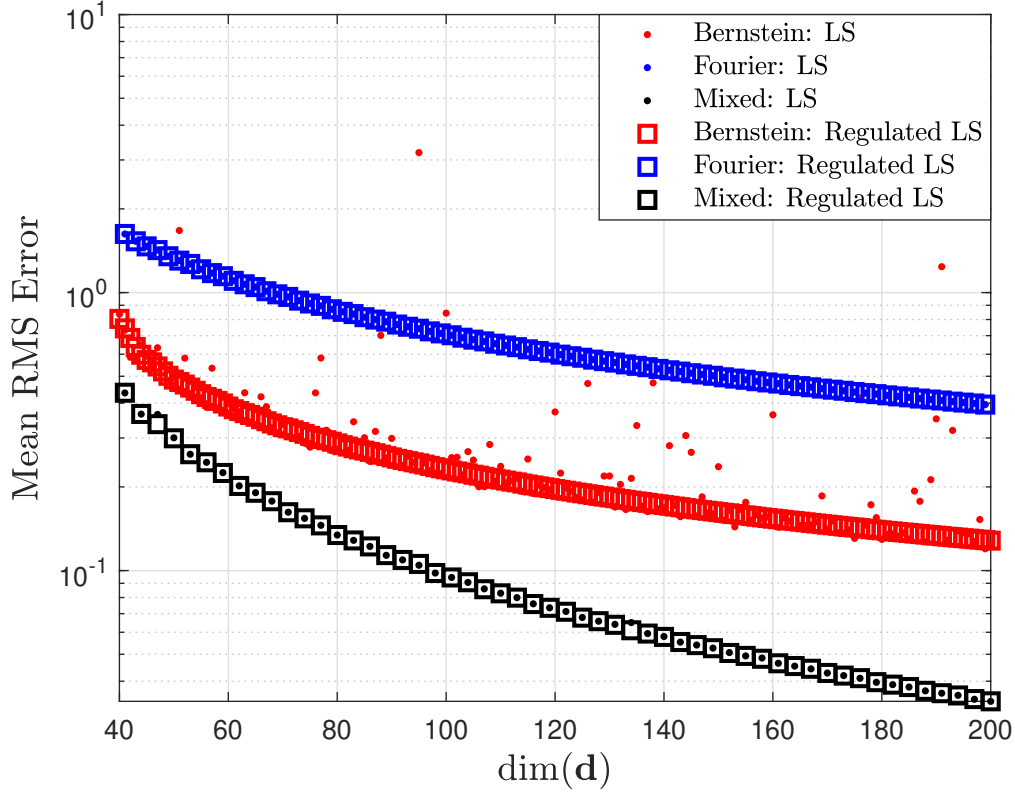


**Figure 3** The mean of the RMS error with respect to time using Bernstein-only (red), Fourier-only (blue), and mixed basis (black) approximants, with coefficients provided by the LS solution (dots) and the regulated LS solution (squares) when  $\lambda = 10^{-14}$ .

the feasibility and consistency of the approximated problem.

### A. Problem Formulation

The optimal motion planning problem can be formulated as follows.

**Problem 1** (Problem *P*). Find  $\mathbf{x}(t) : [0, 1] \rightarrow \mathbb{R}^{m_x}$  and  $\mathbf{u}(t) : [0, 1] \rightarrow \mathbb{R}^{m_u}$  that minimize

$$J(\mathbf{x}(t), \mathbf{u}(t)) = E(\mathbf{x}(0), \mathbf{x}(1)) + \int_0^1 F(\mathbf{x}(t), \mathbf{u}(t)) dt \quad (45)$$

subject to

$$\dot{\mathbf{x}} = \mathbf{f}(\mathbf{x}(t), \mathbf{u}(t)), \quad \forall t \in [0, 1] \quad (46)$$

$$\mathbf{e}(\mathbf{x}(0), \mathbf{x}(1)) = 0 \quad (47)$$

$$\mathbf{h}(\mathbf{x}(t), \mathbf{u}(t)) \leq 0, \quad \forall t \in [0, 1] \quad (48)$$

where  $J : \mathbb{R}^{m_x} \times \mathbb{R}^{m_u} \rightarrow \mathbb{R}$ ,  $E : \mathbb{R}^{m_x} \times \mathbb{R}^{m_x} \rightarrow \mathbb{R}$ ,  $F : \mathbb{R}^{m_x} \times \mathbb{R}^{m_u} \rightarrow \mathbb{R}$ ,  $\mathbf{f} : \mathbb{R}^{m_x} \times \mathbb{R}^{m_u} \rightarrow \mathbb{R}^{m_x}$ ,  $\mathbf{e} : \mathbb{R}^{m_x} \times \mathbb{R}^{m_x} \rightarrow \mathbb{R}^{m_e}$ , and  $\mathbf{h} : \mathbb{R}^{m_x} \times \mathbb{R}^{m_u} \rightarrow \mathbb{R}^{m_h}$ .

The solution to this problem is generally intractable; therefore, we aim to approximate it.

We use equidistant time nodes  $t_k = \frac{k}{n_t}$ ,  $k = 0, \dots, n_t$ , where  $n_t \in \mathbb{N}$ . The mixed approximants are comprised of both Bernstein polynomials and Fourier series to approximate the state and control trajectories:

$$\mathbf{x}_n(t) = \sum_{k=0}^{n_B} \bar{\mathbf{c}}_{x,k} b_{k,n}(t) + \frac{\mathbf{a}_{x,0}}{2} + \sum_{k=1}^{n_F} [\mathbf{a}_{x,k} \cos(2\pi kt) + \mathbf{b}_{x,k} \sin(2\pi kt)] \quad (49)$$

$$\mathbf{u}_n(t) = \sum_{k=0}^{n_B} \bar{\mathbf{c}}_{u,k} b_{k,n}(t) + \frac{\mathbf{a}_{u,0}}{2} + \sum_{k=1}^{n_F} [\mathbf{a}_{u,k} \cos(2\pi kt) + \mathbf{b}_{u,k} \sin(2\pi kt)], \quad (50)$$

where  $\mathbf{x}_n(t) : [0, 1] \rightarrow \mathbb{R}^{m_x}$ ,  $\mathbf{u}_n(t) : [0, 1] \rightarrow \mathbb{R}^{m_u}$ ,  $n_B \in \mathbb{N}$  and  $n_F \in \mathbb{N}$  are the order of approximation of the Bernstein and Fourier basis functions, respectively, and  $n \triangleq \min(n_t, n_B, n_F)$ . Note that the maximal dimension of the decision vector is  $(n_B + 2n_F + 2)(m_x + m_u) + 1$ , which is independent of  $n_t$ .

**Remark 4.** *Choosing  $n_t$  is crucial for the performance of the suggested method. Although the dimension of the decision vector is independent of  $n_t$ , it still affects the performance. If we set  $n_t$  to be too large, we will have numerical problems as the matrix of the basis functions becomes ill-conditioned. In contrast, if  $n_t$  is too small, we can face sampling problems such as aliasing [24]. Therefore, we can easily overcome this challenge by obeying the guidelines of the Nyquist-Shannon sampling theorem and ensuring that  $n_t > 2n_F$ . An appropriate initial value can be  $n_t = n_B$ , as implemented in the Bernstein-only case [5, 10].*

With these approximants, we can formulate the following NLP problem.

**Problem 2** (Problem  $P_n$ ). *Find  $\mathbf{x}_n(t_k)$  and  $\mathbf{u}_n(t_k)$  that minimize*

$$J_n(\mathbf{x}_n(t_k), \mathbf{u}_n(t_k)) = E(\mathbf{x}_n(0), \mathbf{x}_n(1)) + w \sum_{k=0}^{n_t} F(\mathbf{x}_n(t_k), \mathbf{u}_n(t_k)) \quad (51)$$

*subject to*

$$\|\dot{\mathbf{x}}_n(t_k) - \mathbf{f}(\mathbf{x}_n(t_k), \mathbf{u}_n(t_k))\| \leq \delta_P^n, \quad \forall k = 0, \dots, n_t \quad (52)$$

$$\|\mathbf{e}(\mathbf{x}_n(0), \mathbf{x}_n(1))\| \leq \delta_P^n \quad (53)$$

$$\mathbf{h}(\mathbf{x}_n(t_k), \mathbf{u}_n(t_k)) \leq \delta_P^n \cdot \mathbf{I}, \quad \forall k = 0, \dots, n_t \quad (54)$$

where  $w = \frac{1}{n_t+1}$ .

## B. Analysis

This section addresses the feasibility and consistency issues of Problem  $P_n$ , following the lines of analysis presented in [5] for approximations using only Bernstein polynomials. We first make the following assumptions regarding Problem  $P$ .

**Assumption 1.** *The functions  $E, F, \mathbf{f}, \mathbf{e}$ , and  $\mathbf{h}$  are Lipschitz continuous with respect to their arguments.*

**Assumption 2.** *Problem  $P$  admits an optimal solution  $(\mathbf{x}^*(t), \mathbf{u}^*(t))$  that satisfies  $\mathbf{x}^*(t) \in C_{m_x}^1$  and  $\mathbf{u}^*(t) \in C_{m_u}^0$  on  $[0, 1]$ .*

The following theorem summarizes the feasibility result of the primal problem.

**Theorem IV.1** (Feasibility). *Let  $(\mathbf{x}(t), \mathbf{u}(t))$  be a feasible solution to Problem  $P$ , which exists by assumption. Let*

$$\delta_P^n = C_P \max\{\delta_{\dot{\mathbf{x}}}^n, \delta_{\mathbf{x}}^n, \delta_{\mathbf{u}}^n\} \quad (55)$$

where  $C_P$  is a positive constant independent of  $n_B$ ,  $n_F$ , and  $n_t$ . Then, Problem  $P_n$  admits a feasible solution  $(\mathbf{x}_n, \mathbf{u}_n)$  for an arbitrary  $n \in \mathbb{Z}^+$ .

The proof is deferred to Appendix A.

Proving the consistency of the solution requires an additional assumption that ensures the convergence of the approximated solution.

**Assumption 3.** *There exist  $\mathbf{x}^\infty(t) \in C_{m_x}^1$  and  $\mathbf{u}^\infty(t) \in C_{m_u}^0$  on  $[0, 1]$  such that*

$$\lim_{n \rightarrow \infty} (\mathbf{x}_n(t), \mathbf{u}_n(t)) = (\mathbf{x}^\infty(t), \mathbf{u}^\infty(t)). \quad (56)$$

**Theorem IV.2.** *The sequence of optimal solutions to Problem  $P_n$  satisfying Assumption 3 also satisfies*

$$\lim_{n \rightarrow \infty} (\mathbf{x}_n(t), \mathbf{u}_n(t)) = (\mathbf{x}^*(t), \mathbf{u}^*(t)). \quad (57)$$

The proof is deferred to Appendix B.

## V. Necessary Conditions for Optimal Motion Planning

This section presents the theoretical results related to the dual problems of Problem  $P$  and Problem  $P_n$ , following the guidelines of [10].

### A. Problem Formulation

#### 1. Applying PMP to Problem $P$

First, we derive the first-order necessary conditions for Problem  $P$ . Let  $\lambda(t) : [0, 1] \rightarrow \mathbb{R}^{m_x}$  be the trajectory costate, and let  $\boldsymbol{\mu}(t) : [0, 1] \rightarrow \mathbb{R}^{m_h}$  and  $\boldsymbol{\nu} \in \mathbb{R}^{m_e}$  be the multipliers for the inequality and equality constraints, respectively. We define the Lagrangian of the Hamiltonian [25]:

$$\mathcal{L}(\mathbf{x}(t), \mathbf{u}(t), \lambda(t), \boldsymbol{\mu}(t)) = \mathcal{H}(\mathbf{x}(t), \mathbf{u}(t), \lambda(t)) + \boldsymbol{\mu}^T(t) \mathbf{h}(\mathbf{x}(t), \mathbf{u}(t)), \quad (58)$$

where the Hamiltonian is

$$\mathcal{H}(\mathbf{x}(t), \mathbf{u}(t), \boldsymbol{\lambda}(t)) = F(\mathbf{x}(t), \mathbf{u}(t)) + \boldsymbol{\lambda}^T(t) \mathbf{f}(\mathbf{x}(t), \mathbf{u}(t)). \quad (59)$$

The dual problem is formulated as follows [25].

**Problem 3** (Problem  $P_\lambda$ ). *Determine  $\mathbf{x}(t)$ ,  $\mathbf{u}(t)$ ,  $\boldsymbol{\lambda}(t)$ ,  $\boldsymbol{\mu}(t)$ , and  $\mathbf{v}$  that for all  $t \in [0, 1]$  satisfy Eqs. (46)–(48) and*

$$\boldsymbol{\mu}^T(t) \mathbf{h}(\mathbf{x}(t), \mathbf{u}(t)) = 0, \quad \boldsymbol{\mu}(t) \geq 0, \quad (60)$$

$$\dot{\boldsymbol{\lambda}}^T(t) + \mathcal{L}_x(\mathbf{x}(t), \mathbf{u}(t), \boldsymbol{\lambda}(t), \boldsymbol{\mu}(t)) = 0, \quad (61)$$

$$\boldsymbol{\lambda}^T(0) = -\mathbf{v}^T \mathbf{e}_{x(0)}(\mathbf{x}(0), \mathbf{x}(1)) - E_{x(0)}(\mathbf{x}(0), \mathbf{x}(1)), \quad (62)$$

$$\boldsymbol{\lambda}^T(1) = \mathbf{v}^T \mathbf{e}_{x(1)}(\mathbf{x}(0), \mathbf{x}(1)) + E_{x(1)}(\mathbf{x}(0), \mathbf{x}(1)), \quad (63)$$

$$\mathcal{L}_u(\mathbf{x}(t), \mathbf{u}(t), \boldsymbol{\lambda}(t), \boldsymbol{\mu}(t)) = 0. \quad (64)$$

The subscripts are used to denote partial derivatives, e.g.,  $\mathbf{h}_x(\mathbf{x}(t), \mathbf{u}(t)) = \frac{\partial}{\partial \mathbf{x}} \mathbf{h}(\mathbf{x}(t), \mathbf{u}(t))$ .

## 2. KKT Conditions of Problem $P_n$

We derive the necessary conditions of Problem  $P_n$ . We first introduce the approximation of the trajectory costates and the inequality multipliers:

$$\boldsymbol{\lambda}_n(t) = \sum_{k=0}^{n_B} \bar{\mathbf{c}}_{\lambda,k} b_{k,n}(t) + \frac{\mathbf{a}_{\lambda,0}}{2} + \sum_{k=1}^{n_F} [\mathbf{a}_{\lambda,k} \cos(2\pi kt) + \mathbf{b}_{\lambda,k} \sin(2\pi kt)] \quad (65)$$

$$\boldsymbol{\mu}_n(t) = \sum_{k=0}^{n_B} \bar{\mathbf{c}}_{\mu,k} b_{k,n}(t) + \frac{\mathbf{a}_{\mu,0}}{2} + \sum_{k=1}^{n_F} [\mathbf{a}_{\mu,k} \cos(2\pi kt) + \mathbf{b}_{\mu,k} \sin(2\pi kt)], \quad (66)$$

where  $\boldsymbol{\lambda}_n(t) : [0, 1] \rightarrow \mathbb{R}^{m_x}$ , and  $\boldsymbol{\mu}_n(t) : [0, 1] \rightarrow \mathbb{R}^{m_h}$  are the mixed Bernstein-Fourier approximations of  $\boldsymbol{\lambda}(t)$  and  $\boldsymbol{\mu}(t)$ , respectively.

Using these notations, we present the Lagrangian of Problem  $P_n$

$$\begin{aligned} \mathcal{L}_n = & E(\mathbf{x}_n(0), \mathbf{x}_n(1)) + w \sum_{k=0}^{n_t} F(\mathbf{x}_n(t_k), \mathbf{u}_n(t_k)) + \bar{\mathbf{v}}^T \mathbf{e}(\mathbf{x}_n(0), \mathbf{x}_n(1)) \\ & + \sum_{k=0}^{n_t} \lambda_n^T(t_k) (-\dot{\mathbf{x}}_n(t_k) + \mathbf{f}(\mathbf{x}_n(t_k), \mathbf{u}_n(t_k))) + \sum_{k=0}^{n_t} \mu_n^T(t_k) \mathbf{h}(\mathbf{x}_n(t_k), \mathbf{u}_n(t_k)) \end{aligned} \quad (67)$$

where  $\bar{\mathbf{v}} \in \mathbb{R}^{m_e}$ .

Now, we can formulate the dual problem of Problem  $P_n$ .

**Problem 4** (Problem  $P_{n\lambda}$ ). Find  $\mathbf{x}_n(t_k)$ ,  $\mathbf{u}_n(t_k)$ ,  $\lambda_n(t_k)$ ,  $\mu_n(t_k)$ ,  $\bar{\mathbf{v}}$ , and possibly  $t_n$  that satisfy the primal feasibility conditions in Eqs. (52)–(54), the complementary slackness and dual feasibility conditions

$$\left\| \mu_n^T(t_k) \mathbf{h}(\mathbf{x}_n(t_k), \mathbf{u}_n(t_k)) \right\| \leq \frac{\delta_D}{n_t}, \quad \mu_n(t_k) \geq -\frac{\delta_D}{n_t} \mathbf{1}, \quad \forall k = 0, \dots, n_t, \quad (68)$$

the stationarity conditions

$$\begin{aligned} \left\| \frac{\partial \mathcal{L}_n}{\partial \bar{\mathbf{c}}_{x,k}} \right\| &\leq \delta_D, & \left\| \frac{\partial \mathcal{L}_n}{\partial \mathbf{a}_{x,k}} \right\| &\leq \delta_D, & \left\| \frac{\partial \mathcal{L}_n}{\partial \mathbf{b}_{x,k}} \right\| &\leq \delta_D, \\ \left\| \frac{\partial \mathcal{L}_n}{\partial \bar{\mathbf{c}}_{u,k}} \right\| &\leq \delta_D, & \left\| \frac{\partial \mathcal{L}_n}{\partial \mathbf{a}_{u,k}} \right\| &\leq \delta_D, & \left\| \frac{\partial \mathcal{L}_n}{\partial \mathbf{b}_{u,k}} \right\| &\leq \delta_D, \quad \forall k = 0, \dots, n, \end{aligned} \quad (69)$$

and the closure conditions

$$\left\| \frac{\lambda_n^T(0)}{w} + \bar{\mathbf{v}}^T \mathbf{e}_{x(0)}(\mathbf{x}_n(0), \mathbf{x}_n(1)) + E_{x(0)}(\mathbf{x}_n(0), \mathbf{x}_n(1)) \right\| \leq \delta_D, \quad (70)$$

$$\left\| \frac{\lambda_n^T(1)}{w} - \bar{\mathbf{v}}^T \mathbf{e}_{x(1)}(\mathbf{x}_n(0), \mathbf{x}_n(1)) - E_{x(1)}(\mathbf{x}_n(0), \mathbf{x}_n(1)) \right\| \leq \delta_D, \quad (71)$$

where  $\delta_D$  is a small positive number that depends on  $n$  and satisfies  $\lim_{n \rightarrow \infty} \delta_D = 0$ .

**Remark 5.** The closure conditions must be added to Problem  $P_{n\lambda}$  to obtain a consistent approximation of Problem  $P_\lambda$ . These conditions come from the transversality conditions in Eqs. (62)–(63), which do not appear in the KKT conditions of Problem  $P_n$ . More information regarding these conditions

can be found in [8, 26].

## B. Analysis of the Dual Problems

This section analyzes the feasibility and consistency of Problem  $P_{n\lambda}$ . We first show the existence of a solution to this problem, and then we investigate its convergence properties when  $n \rightarrow \infty$ . This yields the covector mapping theorem for the mixed Bernstein-Fourier approximants summarized in Fig 4, which relates the solutions to the different Problems presented in this paper.

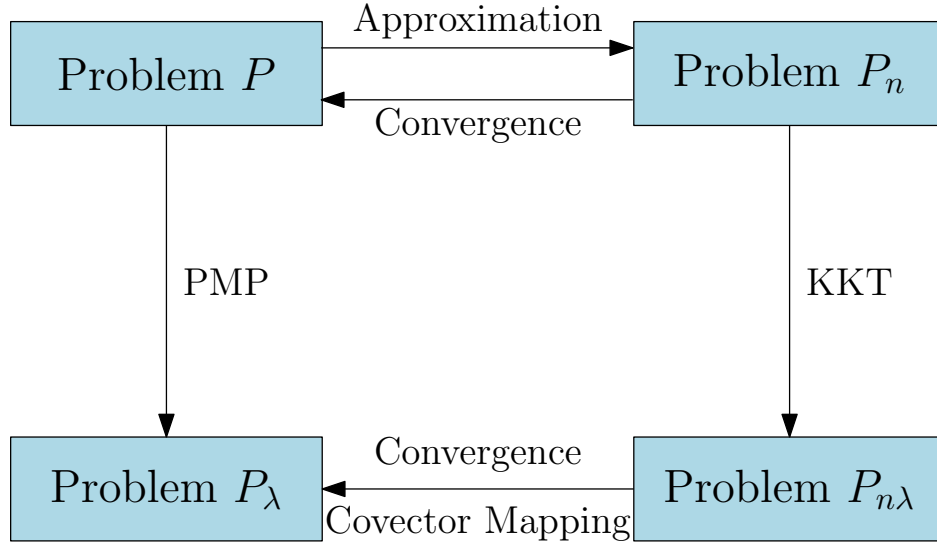


**Figure 4** Schematic overview of the Covector Mapping Theorem for the mixed Bernstein-Fourier approximants

We begin by making the following assumptions regarding Problem  $P_\lambda$ :

**Assumption 4.** *The functions  $E, F, \mathbf{f}, \mathbf{e}$ , and  $\mathbf{h}$  are continuously differentiable with respect to their arguments, and their gradients are Lipschitz continuous over the domain.*

**Assumption 5.** *Problem  $P_\lambda$  admits an optimal solution  $(\mathbf{x}^*(t), \mathbf{u}^*(t), \boldsymbol{\lambda}^*(t), \boldsymbol{\mu}^*(t), \mathbf{v}^*)$  that satisfies  $\mathbf{x}^*(t) \in C_{m_x}^1$ ,  $\mathbf{u}^*(t) \in C_{m_u}^0$ ,  $\boldsymbol{\lambda}^*(t) \in C_{m_\lambda}^1$ ,  $\boldsymbol{\mu}^*(t) \in C_{m_h}^0$  on  $[0, 1]$ , and  $\mathbf{v}^* \in \mathbb{R}^{m_e}$ .*

**Assumption 6.** *The inequality constraint function  $\mathbf{h}(\mathbf{x}(t), \mathbf{u}(t))$  does not contain pure state constraints.*

Note that these assumptions are more restrictive than the ones in Sec. IV. Therefore, some problems which can be solved directly cannot be analyzed using the results of this section. For

example, the numerical problem in Sec. VI.A can be solved directly. It violates Assumption 6, however, so we cannot verify that the solution satisfies the necessary conditions of Problem  $P_\lambda$  because the costates become discontinuous.

**Theorem V.1** (Feasibility of Problem  $P_{n\lambda}$ ). *Let  $(\mathbf{x}(t), \mathbf{u}(t), \boldsymbol{\lambda}(t), \boldsymbol{\mu}(t), \mathbf{v})$  be a feasible solution to Problem  $P_\lambda$ , which exists by assumption. Let  $\delta_P$  be as in (55), and*

$$\delta_D = C_D \max \left\{ \delta_x^n, \delta_u^n, \delta_\lambda^n, \delta_\mu^n, \frac{1}{\sqrt{n}} \right\} \quad (72)$$

where  $C_D$  is a positive constant independent of  $n_B$ ,  $n_F$ , and  $n_t$ . Problem  $P_{n\lambda}$  then admits a feasible solution  $(\mathbf{x}_n, \mathbf{u}_n, \boldsymbol{\lambda}_n, \boldsymbol{\mu}_n, \bar{\mathbf{v}})$  for an arbitrary  $n \in \mathbb{Z}^+$ .

The proof is deferred to Appendix C.

Proving the consistency of the solution requires an additional assumption that ensures the convergence of the approximated solution.

**Assumption 7.** *There exist  $\mathbf{x}^\infty(t) \in C_{m_x}^1$ ,  $\mathbf{u}^\infty(t) \in C_{m_u}^0$ ,  $\boldsymbol{\lambda}^\infty(t) \in C_{m_\lambda}^1$ ,  $\boldsymbol{\mu}^\infty(t) \in C_{m_\mu}^0$  on  $[0, 1]$ , and  $\bar{\mathbf{v}}^\infty \in \mathbb{R}^{m_e}$ , such that*

$$\lim_{n \rightarrow \infty} \left( \mathbf{x}_n(t), \mathbf{u}_n(t), \frac{\boldsymbol{\lambda}_n(t)}{w}, \frac{\boldsymbol{\mu}_n(t)}{w}, \bar{\mathbf{v}} \right) = (\mathbf{x}^\infty(t), \mathbf{u}^\infty(t), \boldsymbol{\lambda}^\infty(t), \boldsymbol{\mu}^\infty(t), \bar{\mathbf{v}}^\infty), \quad \forall t \in [0, 1]. \quad (73)$$

**Theorem V.2.** *The limit of the sequence of optimal solutions to Problem  $P_{n\lambda}$  satisfying Assumption 7 is a solution to Problem  $P_\lambda$ .*

The proof is deferred to Appendix D.

**Theorem V.3** (Covector Mapping Theorem). *Let  $\{\mathbf{x}^*(t), \mathbf{u}^*(t), \boldsymbol{\lambda}^*(t), \boldsymbol{\mu}^*(t), \mathbf{v}^*\}$  and  $\left\{ \mathbf{x}_n^*(t), \mathbf{u}_n^*(t), \frac{\boldsymbol{\lambda}_n^*(t)}{w}, \frac{\boldsymbol{\mu}_n^*(t)}{w}, \bar{\mathbf{v}}^* \right\}$  be the optimal solutions to Problem  $P_\lambda$  and Problem  $P_{n\lambda}$ , respectively. Hence, when  $n \rightarrow \infty$ , the covector mapping*

$$\begin{aligned} \mathbf{x}_n^*(t) &\rightarrow \mathbf{x}^*(t), & \mathbf{u}_n^*(t) &\rightarrow \mathbf{u}^*(t), \\ \frac{\boldsymbol{\lambda}_n^*(t)}{w} &\rightarrow \boldsymbol{\lambda}^*(t), & \frac{\boldsymbol{\mu}_n^*(t)}{w} &\rightarrow \boldsymbol{\mu}^*(t), & \bar{\mathbf{v}}^* &\rightarrow \mathbf{v}^* \end{aligned} \quad (74)$$

is a bijective mapping between the solution of Problem  $P_{n\lambda}$  and the solution of Problem  $P_\lambda$ .

*Proof.* This theorem follows directly from Theorems V.1 and V.2, where the optimal solution to Problem  $P_\lambda$  exists by Assumption 5. Thus, Theorem V.1 shows that  $\{\mathbf{x}^*(t), \mathbf{u}^*(t), w\lambda^*(t), w\boldsymbol{\mu}^*(t), \mathbf{v}^*\}$  is a solution to Problem  $P_{n\lambda}$  which can be constructed using Eqs. (49), (50), (65), and (66). Theorem V.2 shows that the optimal solution of Problem  $P_{n\lambda}$  converges to a solution to Problem  $P_\lambda$ .  $\square$

## VI. Numerical Examples

This section presents two illustrative examples that show the benefits of the proposed solution in this paper. We use MATLAB<sup>®</sup>'s built-in *fmincon* function as an off-the-shelf numerical solver to solve the NLP problem.

### A. Optimization of Observer Trajectory

We address the problem of finding optimal trajectories for localizing a stationary target using an unmanned aerial vehicle (UAV) equipped with bearing-only measurements in three-dimensional scenarios, as presented in [17].

#### 1. Scenario Details

The UAV is assumed to maintain a fixed altitude and constant speed. Hence, it has the following equations of motion:

$$\dot{x}_A(t) = V \cos \psi(t), \quad (75a)$$

$$\dot{y}_A(t) = V \sin \psi(t), \quad (75b)$$

$$\dot{z}_A(t) = 0, \quad (75c)$$

where  $(x_A, y_A, z_A)$  is the UAV's position,  $\psi$  is its heading angle, and  $V$  is its speed. The UAV is assumed to have an onboard vision system that provides the following elevation angle,  $\alpha$ , and

azimuth angle,  $\beta$ , from the UAV to the target:

$$\begin{bmatrix} \alpha_k \\ \beta_k \end{bmatrix} = \mathbf{g}_k + \boldsymbol{\omega}_k = \begin{bmatrix} \tan^{-1} \left( \frac{\Delta z_k}{\sqrt{\Delta x_k^2 + \Delta y_k^2}} \right) \\ \tan^{-1} \left( \frac{\Delta y_k}{\Delta x_k} \right) - \psi_k \end{bmatrix} + \boldsymbol{\omega}_k \quad (76)$$

where  $(\Delta x_k, \Delta y_k, \Delta z_k)$  is the position of the target, which is assumed to be time-invariant, relative to the UAV at  $t_k$ ,  $\{\boldsymbol{\omega}_k\}_{k=1}^f$  is a zero-mean white Gaussian noise sequence with a known constant covariance matrix  $\Sigma$ , and  $t_f$  is the given final time of the scenario.

The main objective of this example is to generate a trajectory that maximizes the information about the target's location obtained from the bearing-only measurements. We also add a 100 m no-fly zone around the target to reduce the detection probability of the UAV. Note that this constraint violates Assumption 6, thus we cannot apply the approximated version of the PMP on this example. Selecting an objective function to maximize the information gathered along a trajectory is nontrivial because it is difficult to quantify this information. We follow the practice of [17], therefore, and use the trace of the Cramér–Rao lower bound (CRLB) to improve the data collected by the UAV regarding the target. The CRLB is computed as the inverse of the celebrated Fisher information matrix (FIM), which satisfies in this case:

$$J_k = \sum_{k=0}^f (G_k)^T \Sigma^{-1} G_k. \quad (77)$$

where  $G_k$  is the Jacobian matrix of  $\mathbf{g}_k$ .

In addition to the no-fly zone described above, the other scenario parameters are as follows. Its duration is set to be 60 s. The UAV starts its motion at  $\begin{bmatrix} 0 & 0 & 20 \end{bmatrix}^T$  m with a constant speed of 30 m/s, heading towards the x-axis. The stationary target is located at  $\begin{bmatrix} 400 & 0 & 0 \end{bmatrix}^T$  m. The UAV's vision system measures the angles to detected objects within its field of view at a frequency of 10 Hz, which yields 600 equally spaced time steps for this scenario. The measurement noise covariance matrices are assumed to be time-invariant, satisfying  $\Sigma = \text{diag}\{(3 \cdot 10^{-3})^2, (3 \cdot 10^{-3})^2\}$ .

## 2. Results

We now present the numerical solutions to the above problem. We set  $n_B = 70$  and  $n_F = 12$ , i.e., we use  $70^{\text{th}}$  order Bernstein polynomials and  $12^{\text{th}}$  order Fourier series to construct candidate UAV trajectories using  $n_t = N_B = 70$ . Because we need to determine the horizontal position,  $(x_A, y_A)$ , and the heading of the UAV at each time step, the state vector has three entries. Therefore, the decision vector has 288 decision variables (71 from the Bernstein part and 25 from the Fourier part of the approximation, for each of the three states) to be determined by the solver. For comparison, we also used a regular Bernstein-based solver, as presented in [5]. The current study indicates that Bernstein approximants of at least  $282^{\text{nd}}$  order are required for the *fmincon* function to converge when the number of function evaluations is limited to a million. Note that this is almost three times more than the number of variables used by the proposed mixed approximation, as the total length of the decision vector is 846. Additionally, Bernstein-only approximants achieve safety constraints only asymptotically. Consequently, based on our simulation results, we extended the no-flight zone radius to 112 m for these approximants.

We initialize both solutions using the same Bernstein coefficients, meaning that the Fourier part of the mixed solution is inactive. It corresponds to a path that directly flies toward the target until it reaches the no-flight zone's boundary and then encircles the target's position. Fig. 5 presents a top view of the optimal trajectories calculated by the NLP solver. For all trajectories, the UAV flies toward the target's location and starts orbiting the no-flight zone, similar to the initial guess. However, when using the mixed Bernstein-Fourier approximation, the UAV is able to follow the no-fly zone boundary much closer. Moreover, the mixed Bernstein-Fourier approximation produces a value of  $6.76 \cdot 10^{-4}$  for the trace of the CRLB, while the Bernstein-based approximation produces a value of  $7.23 \cdot 10^{-4}$ , a nearly 7% performance degradation despite using three times more decision variables. Finally, to show the consistency of the mixed Bernstein-Fourier approximation given by Th. IV.2, we include a solution based on a significantly higher order of approximation, with  $n_B = 600$  and  $n_F = 300$ . For this case, the mixed Bernstein-Fourier approximation produces a value of  $6.64 \cdot 10^{-4}$  for the trace of the CRLB, a performance improvement of only 1.8% compared to the

lower order mixed approximation.

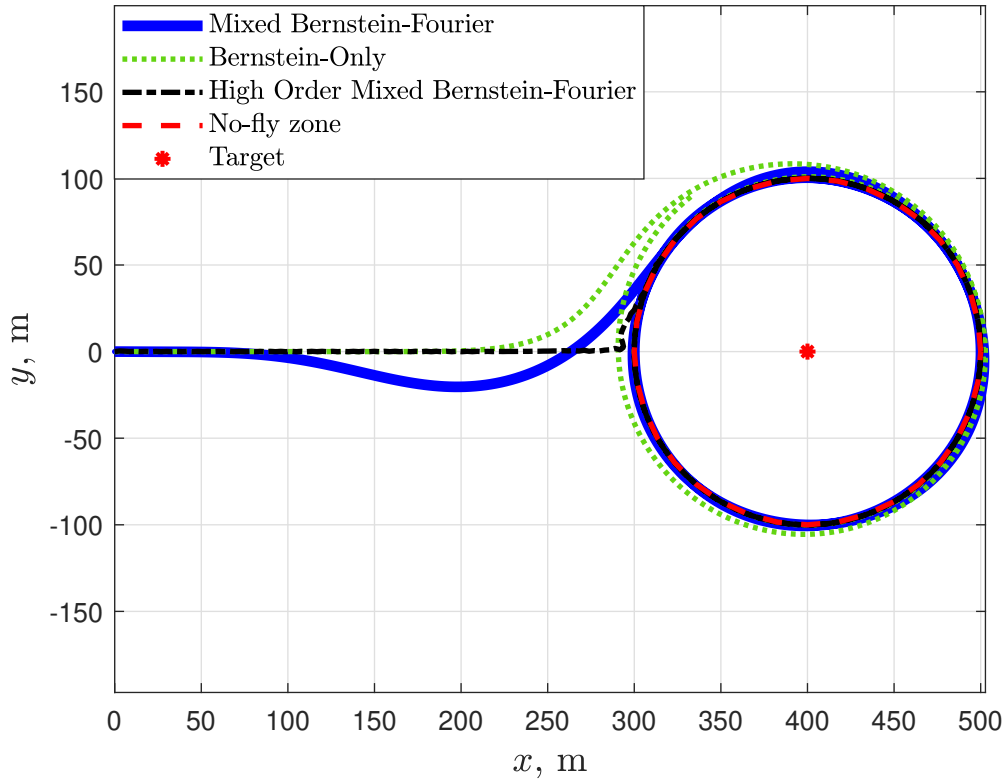


**Figure 5** A top view of optimal UAV trajectories found using different numerical approximations is presented. The blue line denotes the mixed Bernstein-Fourier approximation, and the green line denotes the Bernstein-only approximation, which requires approximately three times more decision variables, resulting in a nearly 7% performance degradation compared to the mixed approximation. The black line denotes a high-order mixed Bernstein-Fourier approximation that illustrates the consistency of these mixed approximations. The red asterisk denotes the target’s stationary position, and the red dashed line denotes the boundary of the no-fly zone.

Fig. 6 presents the optimal solution for the horizontal positioning of the UAV using the mixed Bernstein-Fourier basis functions. The optimal trajectory consists of both periodic and non-periodic components. In the first ten seconds, there is a transient response which is non-periodic. After ten seconds, however, a periodic behavior emerges, exhibiting circular motion with period  $T = 2\pi r/v = 20.94$  s. This periodic behavior matches the known results in [17] for target localization using bearing-only measurements. Note that in [27], similar periodic behaviors appeared for moving target localization using range-only measurements.

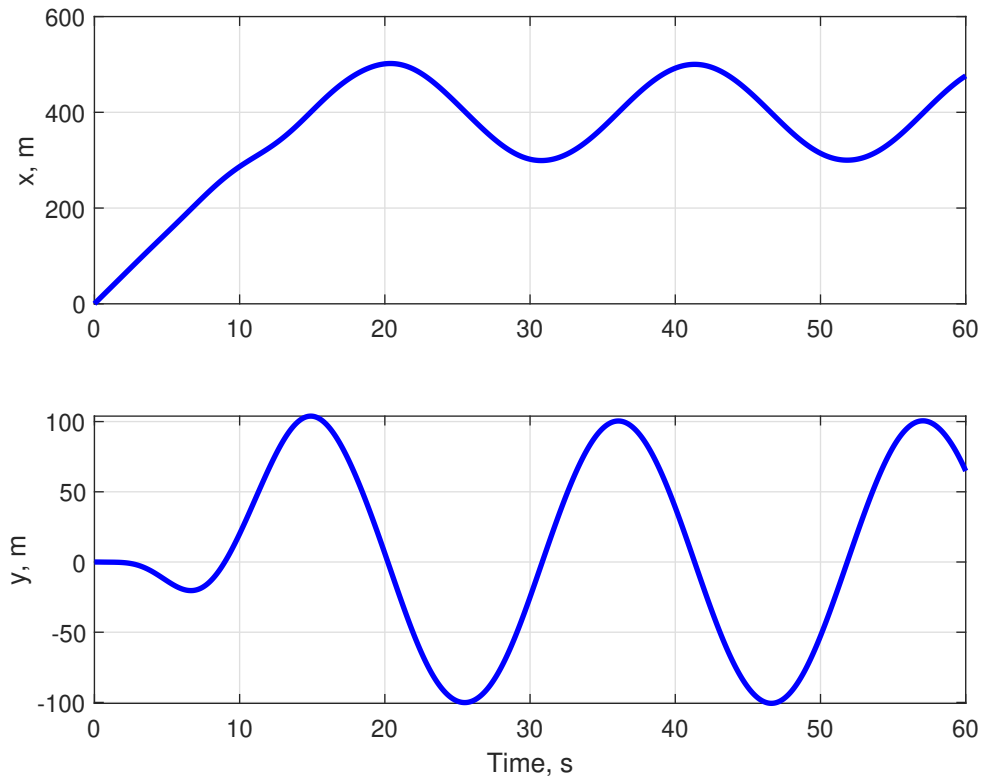


**Figure 6** The optimal motion of the UAV. The upper graph presents the motion in the  $x$ -coordinate direction, and the lower graph presents the motion in the  $y$ -coordinate direction.

### B. Low-Thrust Orbital Transfer

We consider a minimum-effort planar orbital transfer using thrusters that operate continuously and use low thrust to change their course. We use a Cartesian coordinate system that demonstrates the trajectories' periodic behavior.

## 1. Scenario Details

We assume a planar motion model for a vehicle, formulated in normalized units:

$$\dot{x}(t) = v_x(t), \quad (78a)$$

$$\dot{y}(t) = v_y(t), \quad (78b)$$

$$\dot{v}_x(t) = -\frac{x(t)}{r^3(t)} + u_x(t), \quad (78c)$$

$$\dot{v}_y(t) = -\frac{y(t)}{r^3(t)} + u_y(t), \quad (78d)$$

where  $x - y$  are the inertial coordinates,  $v_x$  and  $v_y$  are the velocities in the  $x$  and  $y$  directions, respectively,  $u_x$  and  $u_y$  are the thrust components in the  $x$  and  $y$  directions, respectively, and  $r(t) = \sqrt{x^2(t) + y^2(t)}$  is the radial distance. The initial conditions,  $\left[ x(0), y(0), v_x(0), v_y(0) \right]^T$  are given. We seek to move the vehicle to a different orbit with the final conditions  $\left[ x(t_f), y(t_f), v_x(t_f), v_y(t_f) \right]^T$ , under the thrust component limits

$$|u_x(t)| \leq u^{\max}, \quad |u_y(t)| \leq u^{\max}, \quad \forall t \in [0, t_f]. \quad (79)$$

We also seek to minimize the control effort by selecting the running cost

$$J = \int_0^{t_f} (u_x^2(t) + u_y^2(t)) dt. \quad (80)$$

The nondimensional parameters of the scenario are as follows. Its duration is set to be 80. The vehicle starts its motion in the orbit  $\left[ 1 \ 0 \ 0 \ 1 \right]^T$ , and finishes the transfer in the orbit  $\left[ 4 \ 0 \ 0 \ 0.5 \right]^T$ . The  $u^{\max}$  limit on the thrust components is set to be 0.01.

## 2. Results

We now present the numerical solutions to the low-thrust orbital transfer problem. We set  $n_B = 70$  and  $n_F = 28$ , i.e., we use  $70^{th}$  order Bernstein polynomials and  $28^{th}$  order Fourier series to

construct candidate vehicle trajectories. The approximated trajectories are constructed at equal time intervals of 0.5 s, resulting in 141 time nodes. Because we need to determine the planar position, velocity, and thrust controls at each time step, the state and control vectors have six entries in total. Thus, the decision vector has 768 variables (71 from the Bernstein part and 57 from the Fourier part of the approximation, for each state and controller) to be determined by the solver.

The optimal solution gives a trajectory with a normalized cost of 0.00354. The spatial trajectory is presented in Fig. 7. The trajectory uses six revolutions around the Earth to complete the transfer from initial to final conditions. The optimal trajectories are presented in Fig. 8, which clearly

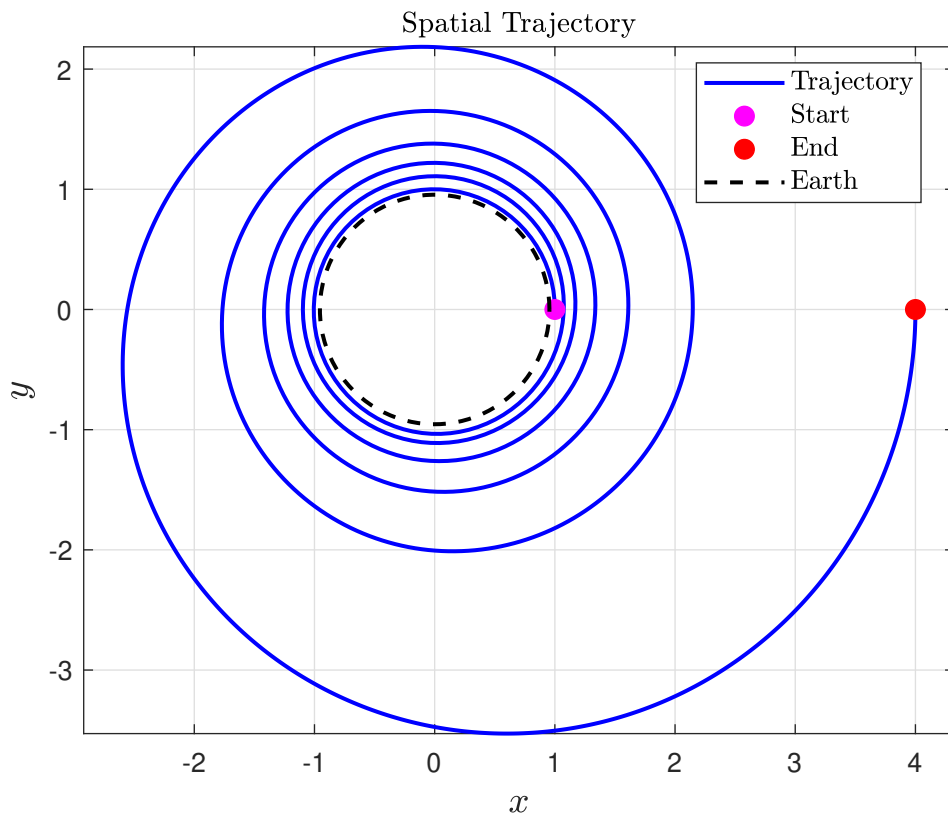


**Figure 7** The optimal spatial trajectory of the vehicle (blue line) from the initial conditions (magenta x) to the final conditions (red x) over the Earth (dashed black line).

demonstrates the periodic behavior of the states and controls. Fig. 8a presents the optimal states of the orbital transfer. The predicted periodic behavior of the orbital motion is evident for both the position and velocity of the vehicle. The optimal controls, presented in Fig. 8b, also show periodic

behavior. However, this behavior is not straightforward and cannot be predicted beforehand.

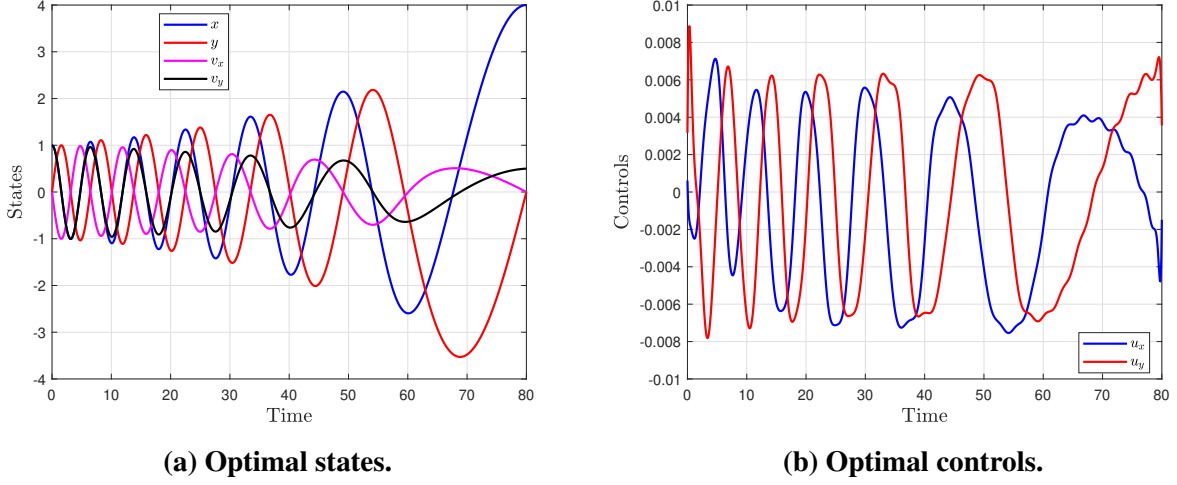


**Figure 8** The optimal trajectories of the vehicle.

We next present the results of the PMP. The Hamiltonian satisfies:

$$H(\mathbf{x}, \mathbf{u}, \boldsymbol{\lambda}) = u_x^2 + u_y^2 + \lambda_x v_x + \lambda_y v_y + \lambda_{v_x} \left( -\frac{x}{r^3} + u_x \right) + \lambda_{v_y} \left( -\frac{y}{r^3} + u_y \right) \quad (81)$$

and the resulting adjoint equations are

$$\dot{\lambda}_x = \left( \frac{1}{r^3} - \frac{3x^2}{r^5} \right) \lambda_{v_x} - \frac{3xy}{r^5} \lambda_{v_y}, \quad (82a)$$

$$\dot{\lambda}_y = -\frac{3xy}{r^5} \lambda_{v_x} + \left( \frac{1}{r^3} - \frac{3y^2}{r^5} \right) \lambda_{v_y}, \quad (82b)$$

$$\dot{\lambda}_{v_x} = -\lambda_x, \quad (82c)$$

$$\dot{\lambda}_{v_y} = -\lambda_y. \quad (82d)$$

Using the covector mapping theorem, the initial conditions for the costates satisfy

$$\boldsymbol{\lambda}(0) = \mathbf{v}_{\mathbf{x}_0}, \quad (83)$$

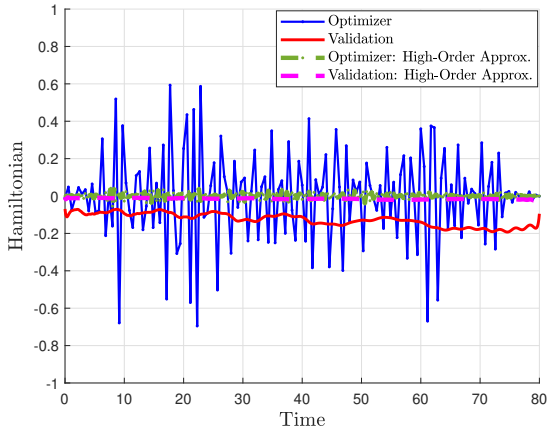
which are used to obtain a numerically propagated solution for the states and costates given in (82).

Using the method presented in [28], the control inputs calculated by the NLP solver were propagated using MATLAB’s Runge-Kutta function to validate the primal and dual variables for our low-thrust orbital transfer problem.

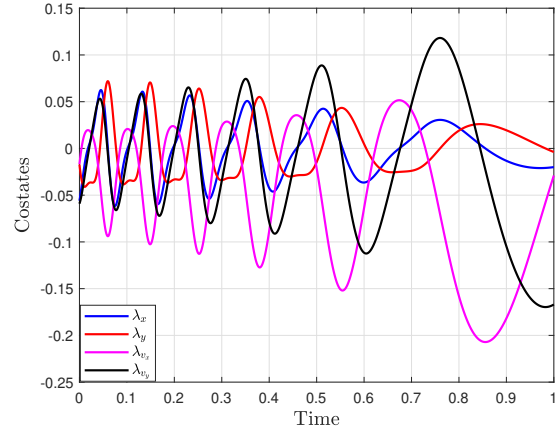
The results of PMP are presented in Fig. 9. The PMP necessary conditions require the Hamiltonian to be constant and equal to zero. The resulting Hamiltonian, plotted in Fig. 9a appears to be nonzero and time varying, which would violate the PMP theory. Therefore, we also include a solution computed using a higher order approximation with double the number of basis functions (resulting in 1548 decision variables):  $n_B = 140$ ,  $n_F = 56$ , and  $n_t = 281$ . This result appears to satisfy the PMP necessary conditions with a cost of 0.00334, an approximately 6% performance improvement obtained by doubling the order of approximation. This graph demonstrates the consistency property presented in Th. V.2. We include the solution obtained directly from the off-the-shelf NLP solver and the solution obtained from the validation process which numerically propagated the costate initial conditions in (83). Thus, we get that the optimized low-order approximation results in a volatile solution, and the solution from the validation has a bias. However, the volatility decreased drastically in the optimized solution for the high-order case, and the bias is removed from the validation. Fig. 9b presents the costates from validating the solution for the low-order case. We can then see that the periodic behavior of the states and controls also translates into periodic behavior of the costates. Note that similar behavior is observed for the high-order case.

## VII. Conclusions

This paper introduced a comprehensive mixed Bernstein-Fourier approximation methodology, significantly advancing approximation theory by effectively combining Bernstein polynomials and Fourier series. We established theoretical results, including explicit proofs of uniform convergence for approximated functions, their derivatives, and integrals. These proofs were accompanied by detailed error bound analyses, which demonstrated the robustness and accuracy of the mixed approximation method. Furthermore, a regulated LS formulation was developed to optimally determine approximation coefficients, enhancing our approach’s practical flexibility and numerical



(a) The Hamiltonian from the NLP solver (blue) and from the validation (red) vs. the high-order approximation results from the NLP solver (green) and the validation (magenta).



(b) The optimal costates of the vehicle:  $\lambda_x$  (blue),  $\lambda_y$  (red),  $\lambda_{v_x}$  (magenta), and  $\lambda_{v_y}$  (black).

**Figure 9 The dual variables of the solution.**

stability.

In addition to theoretical advancements in approximation theory, we applied our mixed Bernstein-Fourier approach to optimal motion planning problems, demonstrating its significant advantages over traditional methods for problems that exhibit periodic behavior. By proving the feasibility and consistency of the approximated optimal control solutions, we established theoretical guarantees on the accuracy of our method. We further extended the covector mapping theorem to the mixed Bernstein-Fourier setting, providing robust theoretical assurances for dual variable approximations, crucial for validating optimality conditions derived from PMP.

Comprehensive numerical examples reinforced these theoretical insights, highlighting substantial improvements in computational efficiency, accuracy, and practical performance. Specifically, our numerical studies illustrated the mixed approach's superior handling of complex periodic dynamics and constraints, achieving high precision with fewer variables than Bernstein-only approximations.

## Acknowledgment

The authors would like to thank the Office of Naval Research Science of Autonomy Program under Grant No. N0001425GI01545 and Consortium for Robotics Unmanned Systems Education and Research at the Naval Postgraduate School for sponsoring this research. This project was also supported in part by an appointment to the NRC Research Associateship Program at the Naval Postgraduate School, administered by the Fellowships Office of the National Academies of Sciences, Engineering, and Medicine.

### A. Proof of Th. IV.1

*Proof.* Our objective is to show that there exist Bernstein and Fourier coefficients and time  $t_n$  such that the constraints of Problem  $P_n$  are satisfied with the given  $\delta_P$ , where there exist  $\mathbf{x}(t)$  and  $\mathbf{u}(t)$  which comprise a feasible solution to Problem  $P$  according to the underlying assumptions. Define equispaced time nodes  $t_k \triangleq \frac{k}{n_t}$  such that  $\mathbf{x}_k$  and  $\mathbf{u}_k$  are defined according to (49) and (50), respectively, whose construction is readily achieved using the coefficients presented in Eqs. (20)–(22). Similarly to (18), the solution of problem P can be presented as:

$$\mathbf{x}(t) = \mathbf{x}_g(t) + \mathbf{x}_p(t), \quad \mathbf{u}(t) = \mathbf{u}_g(t) + \mathbf{u}_p(t) \quad (84)$$

where the subscript  $\mathbf{p}$  denotes the periodic part inside the function, and  $\mathbf{g}$  denotes the nonperiodic part of it.

We first show that the dynamic constraint is satisfied. We add the nulled expression  $\mathbf{f}(\mathbf{x}(t_k), \mathbf{u}(t_k)) - \dot{\mathbf{x}}(t_k)$  from Eq. (46) to get that

$$\begin{aligned} \|\dot{\mathbf{x}}_k - \mathbf{f}(\mathbf{x}_k, \mathbf{u}_k)\| &\leq \|\dot{\mathbf{x}}_k - \dot{\mathbf{x}}(t_k)\| + \|\mathbf{f}(\mathbf{x}(t_k), \mathbf{u}(t_k)) - \mathbf{f}(\mathbf{x}_k, \mathbf{u}_k)\| \leq \\ &C_1 W_{\dot{\mathbf{x}}_g} \left( \frac{1}{\sqrt{n_B}} \right) + \frac{A_1 \log n_F}{n_F^{r-1}} W_{\dot{\mathbf{x}}_p} \left( \frac{2\pi}{n_F} \right) + L_{\mathbf{f}_x} \left[ C_0 W_{\mathbf{x}_g} \left( \frac{1}{\sqrt{n_B}} \right) \frac{A_0 \log n_F}{n_F^r} W_{\mathbf{x}_p} \left( \frac{2\pi}{n_F} \right) \right] \\ &+ L_{\mathbf{f}_u} \left[ \bar{C}_0 W_{\mathbf{u}_g} \left( \frac{1}{\sqrt{n_B}} \right) \frac{\bar{A}_0 \log n_F}{n_F^r} W_{\mathbf{u}_p} \left( \frac{2\pi}{n_F} \right) \right] = \delta_{\dot{\mathbf{x}}}^n + L_{\mathbf{f}_x} \delta_{\mathbf{x}}^n + L_{\mathbf{f}_u} \delta_{\mathbf{u}}^n \end{aligned} \quad (85)$$

where  $A_0, \bar{A}_0, A_1, C_0, \bar{C}_0,$  and  $C_1$  are positive constants independent of  $n_B, n_F,$  and  $n_t$ ;  $W_{\mathbf{x}_g}(\cdot), W_{\dot{\mathbf{x}}_g}(\cdot), W_{\mathbf{x}_p}(\cdot), W_{\dot{\mathbf{x}}_p}(\cdot), W_{\mathbf{u}_g}(\cdot),$  and  $W_{\mathbf{u}_p}(\cdot),$  are moduli of continuity for  $\mathbf{x}_g(t), \dot{\mathbf{x}}_g(t), \mathbf{x}_p(t), \dot{\mathbf{x}}_p(t), \mathbf{u}_g(t),$  and  $\mathbf{u}_p(t),$  respectively; and  $L_{\mathbf{f}_x}$  and  $L_{\mathbf{f}_u}$  are the Lipschitz constants of  $\mathbf{f}$  with respect to  $\mathbf{x}$  and  $\mathbf{u},$  respectively. We set  $C_P > (1 + L_{\mathbf{f}_x} + L_{\mathbf{f}_u})$  such that Eq. (55) holds. The second inequality in (85) holds using Theorem III.1 and Corollary III.1.1. The convergence of  $\delta_P$  to zero follows.

Similarly, the inequality constraint satisfies

$$\|\mathbf{h}(\mathbf{x}_n(t_k), \mathbf{u}_n(t_k)) - \mathbf{h}(\mathbf{x}(t_k), \mathbf{u}(t_k))\| \leq L_{\mathbf{h}_x} \delta_{\mathbf{x}}^n + L_{\mathbf{h}_u} \delta_{\mathbf{u}}^n \quad (86)$$

where  $L_{\mathbf{h}_x}$  and  $L_{\mathbf{h}_u}$  are the Lipschitz constant of  $\mathbf{h}$  with respect to  $\mathbf{x}$  and  $\mathbf{u},$  respectively. Hence,

$$\mathbf{h}(\mathbf{x}_n(t_k), \mathbf{u}_n(t_k)) \leq \mathbf{h}(\mathbf{x}(t_k), \mathbf{u}(t_k)) + (L_{\mathbf{h}_x} \delta_{\mathbf{x}}^n + L_{\mathbf{h}_u} \delta_{\mathbf{u}}^n) \cdot \mathbf{1} \leq (L_{\mathbf{h}_x} \delta_{\mathbf{x}}^n + L_{\mathbf{h}_u} \delta_{\mathbf{u}}^n) \cdot \mathbf{1} \quad (87)$$

where the second inequality holds by using (48) and by setting  $C_P > L_{\mathbf{h}_x} + L_{\mathbf{h}_u}.$

Similarly, for the equality constraint, we add the nulled expression  $\mathbf{e}(\mathbf{x}(0), \mathbf{x}(1))$  from Eq. (47) to the constraints in Eq. (53) to get that

$$\|\mathbf{e}(\mathbf{x}_n(0), \mathbf{x}_n(1)) - \mathbf{e}(\mathbf{x}(0), \mathbf{x}(1))\| \leq L_{\mathbf{e}} \left[ C_0 W_{\mathbf{x}_g} \left( \frac{1}{\sqrt{n_B}} \right) + \frac{A_0 \log n_F}{n_F^r} W_{\mathbf{x}_p} \left( \frac{2\pi}{n_F} \right) \right] = L_{\mathbf{e}} \delta_{\mathbf{x}}^n \quad (88)$$

where  $L_{\mathbf{e}}$  is the Lipschitz constant of  $\mathbf{e}.$  Then, the constraint holds as we set  $C_P > L_{\mathbf{e}}. \quad \square$

## B. Proof of Th. IV.2

*Proof.* The proof is divided into three steps: 1) we show that  $(\mathbf{x}^\infty(t), \mathbf{u}^\infty(t))$  is a feasible solution to Problem  $P$ ; 2) we prove that

$$\lim_{n \rightarrow \infty} J_n(\mathbf{x}_n(t), \mathbf{u}_n(t)) = J(\mathbf{x}^\infty(t), \mathbf{u}^\infty(t)); \quad (89)$$

and 3) we show that  $J(\mathbf{x}^\infty(t), \mathbf{u}^\infty(t)) = J(\mathbf{x}^*(t), \mathbf{u}^*(t)).$

**Step 1)** If  $(\mathbf{x}^\infty(t), \mathbf{u}^\infty(t))$  satisfy the constraints of Problem  $P$ , then it is a feasible solution. First, we show it satisfies the dynamic constraint, that is,

$$\dot{\mathbf{x}}^\infty(t) - \mathbf{f}(\mathbf{x}^\infty(t), \mathbf{u}^\infty(t)) = \mathbf{0}. \quad (90)$$

We prove it by contradiction. Assume that the equality above does not hold, so there exists  $t' \in [0, 1]$  such that

$$\|\dot{\mathbf{x}}^\infty(t') - \mathbf{f}(\mathbf{x}^\infty(t'), \mathbf{u}^\infty(t'))\| > 0. \quad (91)$$

Let  $t_k = \frac{k}{n_t}$ . Because  $\{t_k\}_{k=0}^{n_t}$  is dense in  $[0, 1]$  when  $n_t \rightarrow \infty$ , there exists a subsequence with indices  $\{k_N\}_{N=0}^\infty$  such that

$$\lim_{N \rightarrow \infty} t_{k_N} = t'. \quad (92)$$

Using the continuity of  $\dot{\mathbf{x}}^\infty(t)$  and  $\mathbf{u}^\infty(t)$ , we get that

$$\begin{aligned} \|\dot{\mathbf{x}}^\infty(t') - \mathbf{f}(\mathbf{x}^\infty(t'), \mathbf{u}^\infty(t'))\| &= \lim_{N \rightarrow \infty} \|\dot{\mathbf{x}}^\infty(t_{k_N}) - \mathbf{f}(\mathbf{x}^\infty(t_{k_N}), \mathbf{u}^\infty(t_{k_N}))\| \\ &= \lim_{N \rightarrow \infty} \|\dot{\mathbf{x}}^\infty(t_{k_N}) - \dot{\mathbf{x}}_n(t') + \dot{\mathbf{x}}_n(t') - \mathbf{f}(\mathbf{x}^\infty(t_{k_N}), \mathbf{u}^\infty(t_{k_N}))\| \\ &\leq \lim_{N \rightarrow \infty} \|\dot{\mathbf{x}}^\infty(t_{k_N}) - \dot{\mathbf{x}}_n(t')\| + \lim_{N \rightarrow \infty} \|\dot{\mathbf{x}}_n(t') - \mathbf{f}(\mathbf{x}^\infty(t_{k_N}), \mathbf{u}^\infty(t_{k_N}))\| = 0 \end{aligned} \quad (93)$$

where the first term in the right-hand side of the inequality is zero from the continuity of  $\dot{\mathbf{x}}^\infty$  and the second term converges to zero by using Assumption 3 and because it satisfies Eq. (52). Therefore, we contradict (91) and prove that  $(\mathbf{x}^\infty(t), \mathbf{u}^\infty(t))$  satisfy the dynamic constraint.

Using similar arguments, we can show by contradiction that the inequality constraint in (48) is also satisfied.

The equality constraint in (47) we get by using Assumption 3 and Eq. (53) that

$$\mathbf{e}(\mathbf{x}^\infty(0), \mathbf{x}^\infty(1)) = \lim_{n \rightarrow \infty} \mathbf{e}(\mathbf{x}_n(0), \mathbf{x}_n(1)) = \mathbf{0} \quad (94)$$

as  $\lim_{n \rightarrow \infty} \delta_p^n = 0$ .

**Step 2)** To show that (89) is satisfied, we first need to show that the running cost satisfies

$$\lim_{n \rightarrow \infty} w \sum_{k=0}^{n_t} F(\mathbf{x}_n(t_k), \mathbf{u}_n(t_k)) = \int_0^1 F(\mathbf{x}^\infty(t), \mathbf{u}^\infty(t)) dt. \quad (95)$$

This relation holds using Assumptions 1 and 3 and then applying Theorem III.2.

The following relation regarding the terminal cost also holds using Assumptions 1 and 3

$$\lim_{n \rightarrow \infty} E(\mathbf{x}_n(0), \mathbf{x}_n(1)) = E(\mathbf{x}^\infty(0), \mathbf{x}^\infty(1)). \quad (96)$$

**Step 3)** To show the result of this step we first construct approximants to  $(\mathbf{x}^*(t), \mathbf{u}^*(t))$ , the optimal solution of Problem  $P$ , using the relations in Eqs. (20)–(22). We denote them by  $(\tilde{\mathbf{x}}_n^*(t), \tilde{\mathbf{u}}_n^*(t))$ .

Then, using the same arguments in the previous step, we can show that

$$\lim_{n \rightarrow \infty} J_n(\tilde{\mathbf{x}}_n^*(t), \tilde{\mathbf{u}}_n^*(t)) = J(\mathbf{x}^*(t), \mathbf{u}^*(t)). \quad (97)$$

Having already shown the feasibility of the solution  $(\mathbf{x}^\infty(t), \mathbf{u}^\infty(t))$  to Problem  $P$ , we now use the result of the second step to obtain

$$J(\mathbf{x}^*(t), \mathbf{u}^*(t)) \leq J(\mathbf{x}^\infty(t), \mathbf{u}^\infty(t)) = \lim_{n \rightarrow \infty} J_n(\mathbf{x}_n(t), \mathbf{u}_n(t)). \quad (98)$$

However, Th. IV.1 shows that  $(\mathbf{x}^*(t), \mathbf{u}^*(t))$  is a feasible solution to Problem  $P_n$ , so

$$J(\mathbf{x}^\infty(t), \mathbf{u}^\infty(t)) \leq \lim_{n \rightarrow \infty} J_n(\tilde{\mathbf{x}}_n^*(t), \tilde{\mathbf{u}}_n^*(t)) = J(\mathbf{x}^*(t), \mathbf{u}^*(t)). \quad (99)$$

Thus, using expressions (97) and (99), we get

$$J(\mathbf{x}^*(t), \mathbf{u}^*(t)) \leq J(\mathbf{x}^\infty(t), \mathbf{u}^\infty(t)) \leq J(\mathbf{x}^*(t), \mathbf{u}^*(t)) \quad (100)$$

and the result follows by applying the squeeze theorem.  $\square$

### C. Proof of Th. V.1

*Proof.* Similarly to the proof of Th. IV.1, we construct a feasible solution for Problem  $P_{n\lambda}$  using an existing solution to Problem  $P_\lambda$ . Let  $(\mathbf{x}(t), \mathbf{u}(t), \boldsymbol{\lambda}(t), \boldsymbol{\mu}(t), \boldsymbol{\nu})$  be a feasible solution to Problem  $P_\lambda$ . Define equispaced time nodes  $t_k \triangleq \frac{k}{n_B}$  for all  $k = 0, \dots, n_t$ . The approximated states,  $\mathbf{x}_n(t)$ , and control inputs,  $\mathbf{u}_n(t)$ , satisfy Eq. (49) and (50), respectively, and the approximated costates,  $\boldsymbol{\lambda}_n(t)$ , and inequality multipliers,  $\boldsymbol{\mu}_n(t)$ , satisfy Eq. (65) and (66), respectively, whose construction is readily achieved using the coefficients presented in Eqs. (20)–(22). The equality multipliers satisfy  $\boldsymbol{\nu} = \bar{\boldsymbol{\nu}}$ .

Th. IV.1 shows that  $\mathbf{x}_n(t)$  and  $\mathbf{u}_n(t)$  satisfy Eqs. (52)–(54). The remainder of this proof shows that  $(\mathbf{x}_n(t), \mathbf{u}_n(t), \boldsymbol{\lambda}_n(t), \boldsymbol{\mu}_n(t), \bar{\boldsymbol{\nu}})$  also satisfy Eqs. (68)–(71). First, we define:

$$\bar{\boldsymbol{\lambda}}_n(t_k) = \frac{\boldsymbol{\lambda}_n(t_k)}{w}, \quad \bar{\boldsymbol{\mu}}_n(t_k) = \frac{\boldsymbol{\mu}_n(t_k)}{w} \quad (101)$$

for all  $k = 0, \dots, n_t$ .

We start by showing that the conditions in (68) are satisfied. Using the definition above for  $\bar{\boldsymbol{\mu}}_n(t_k)$ , we add and subtract the expression  $w\boldsymbol{\mu}^T(t_k)(\mathbf{h}(\mathbf{x}_n(t_k), \mathbf{u}_n(t_k)) + \mathbf{h}(\mathbf{x}(t_k), \mathbf{u}(t_k)))$ , so we get

$$\begin{aligned} \|\boldsymbol{\mu}_n^T(t_k)\mathbf{h}(\mathbf{x}_n(t_k), \mathbf{u}_n(t_k))\| &= \|w\bar{\boldsymbol{\mu}}_n^T(t_k)\mathbf{h}(\mathbf{x}_n(t_k), \mathbf{u}_n(t_k))\| \leq w\|\boldsymbol{\mu}^T(t_k)\mathbf{h}(\mathbf{x}(t_k), \mathbf{u}(t_k))\| \\ &+ w\|(\bar{\boldsymbol{\mu}}_n^T(t_k) - \boldsymbol{\mu}^T(t_k))\mathbf{h}(\mathbf{x}_n(t_k), \mathbf{u}_n(t_k))\| + w\|\boldsymbol{\mu}^T(t_k)(\mathbf{h}(\mathbf{x}_n(t_k), \mathbf{u}_n(t_k)) - \mathbf{h}(\mathbf{x}(t_k), \mathbf{u}(t_k)))\| \end{aligned} \quad (102)$$

where the inequality holds by using the triangle inequality. Note that the first expression in the inequality is nulled using (60). Moreover, we get that

$$\|(\bar{\boldsymbol{\mu}}_n^T(t_k) - \boldsymbol{\mu}^T(t_k))\mathbf{h}(\mathbf{x}_n(t_k), \mathbf{u}_n(t_k))\| \leq \delta_\mu^n \mathbf{h}_{\max} \quad (103)$$

$$\|\boldsymbol{\mu}^T(t_k)(\mathbf{h}(\mathbf{x}_n(t_k), \mathbf{u}_n(t_k)) - \mathbf{h}(\mathbf{x}(t_k), \mathbf{u}(t_k)))\| \leq \boldsymbol{\mu}_{\max}(L_{\mathbf{h}_x}\delta_x^n + L_{\mathbf{h}_u}\delta_u^n) \quad (104)$$

where  $L_{\mathbf{h}_x}$  and  $L_{\mathbf{h}_u}$  are the Lipschitz constant of  $\mathbf{h}$  with respect to  $\mathbf{x}$  and  $\mathbf{u}$ , respectively, and  $\mathbf{h}_{\max}$  and  $\boldsymbol{\mu}_{\max}$  are the maximal values for  $\mathbf{h}$  and  $\boldsymbol{\mu}$  on  $[0, 1]$ , respectively, whose existence is guaranteed

from Assumptions 1 and 5. Thus, there exists a positive constant  $\tilde{C}$  that is independent of  $n$ , such that

$$\left\| \boldsymbol{\mu}_n^T(t_k) \mathbf{h}(\mathbf{x}_n(t_k), \mathbf{u}_n(t_k)) \right\| \leq w \tilde{C} \max \left\{ \delta_\mu^n, \delta_x^n, \delta_u^n \right\}, \quad \forall k = 0, \dots, n_t \quad (105)$$

where we choose  $C_D > \tilde{C}$ , thus  $\left\| \boldsymbol{\mu}_n^T(t_k) \mathbf{h}(\mathbf{x}_n(t_k), \mathbf{u}_n(t_k)) \right\|$  converges uniformly as  $n \rightarrow \infty$  using  $\delta_D$  from (72). Similarly, we add and subtract  $w\boldsymbol{\mu}(t_k)$ , and get

$$\boldsymbol{\mu}_n(t_k) = w\bar{\boldsymbol{\mu}}_n(t_k) \geq w\boldsymbol{\mu}(t_k) - w \left\| \boldsymbol{\mu}(t_k) - \bar{\boldsymbol{\mu}}_n(t_k) \right\| \mathbf{1} \geq -w\delta_\mu^n \mathbf{1}, \quad (106)$$

which proves that Eq. (68) holds.

Next, we prove that the stationarity conditions hold. First, we consider

$$\begin{aligned} \left\| \frac{\partial \mathcal{L}_n}{\partial \bar{\mathbf{c}}_{x,0}} \right\| &= \left\| E_{\mathbf{x}(0)}(\mathbf{x}_n(0), \mathbf{x}_n(1)) + w \sum_{k=0}^{n_t} F_x(\mathbf{x}_n(t_k), \mathbf{u}_n(t_k)) b_{0,n}(t_k) + \bar{\mathbf{v}}^T \mathbf{e}_{\mathbf{x}(0)}(\mathbf{x}_n(0), \mathbf{x}_n(1)) \right. \\ &+ \left. \sum_{k=0}^{n_t} \boldsymbol{\lambda}_n^T(t_k) \left( \mathbf{f}_x(\mathbf{x}_n(t_k), \mathbf{u}_n(t_k)) b_{0,n}(t_k) - \dot{b}_{0,n}(t_k) \right) + \sum_{k=0}^{n_t} \boldsymbol{\mu}_n^T(t_k) \mathbf{h}_x(\mathbf{x}_n(t_k), \mathbf{u}_n(t_k)) b_{0,n}(t_k) \right\| \\ &= \left\| E_{\mathbf{x}(0)}(\mathbf{x}_n(0), \mathbf{x}_n(1)) + w \sum_{k=0}^{n_t} F_x(\mathbf{x}_n(t_k), \mathbf{u}_n(t_k)) b_{0,n}(t_k) + \bar{\mathbf{v}}^T \mathbf{e}_{\mathbf{x}(0)}(\mathbf{x}_n(0), \mathbf{x}_n(1)) \right. \\ &+ \left. w \sum_{k=0}^{n_t} \bar{\boldsymbol{\lambda}}_n^T(t_k) \left( \mathbf{f}_x(\mathbf{x}_n(t_k), \mathbf{u}_n(t_k)) b_{0,n}(t_k) - \dot{b}_{0,n}(t_k) \right) + w \sum_{k=0}^{n_t} \bar{\boldsymbol{\mu}}_n^T(t_k) \mathbf{h}_x(\mathbf{x}_n(t_k), \mathbf{u}_n(t_k)) b_{0,n}(t_k) \right\| \end{aligned}$$

where in the second equality we substitute  $\boldsymbol{\lambda}_n^T(t_k) = w\bar{\boldsymbol{\lambda}}_n^T(t_k)$  and  $\boldsymbol{\mu}_n^T(t_k) = w\bar{\boldsymbol{\mu}}_n^T(t_k)$ .

Consider the following inequality where we add and subtract  $\int_0^1 F_x(\mathbf{x}_n(t), \mathbf{u}_n(t)) b_{0,n}(t) dt$ :

$$\begin{aligned} &\left\| w \sum_{k=0}^{n_t} F_x(\mathbf{x}_n(t_k), \mathbf{u}_n(t_k)) b_{0,n}(t_k) - \int_0^1 F_x(\mathbf{x}(t), \mathbf{u}(t)) b_{0,n}(t) dt \right\| \\ &\leq \left\| w \sum_{k=0}^{n_t} F_x(\mathbf{x}_n(t_k), \mathbf{u}_n(t_k)) b_{0,n}(t_k) - \int_0^1 F_x(\mathbf{x}_n(t), \mathbf{u}_n(t)) b_{0,n}(t) dt \right\| \\ &+ \left\| \int_0^1 F_x(\mathbf{x}_n(t), \mathbf{u}_n(t)) b_{0,n}(t) dt - \int_0^1 F_x(\mathbf{x}(t), \mathbf{u}(t)) b_{0,n}(t) dt \right\|. \quad (107) \end{aligned}$$

Using Assumption 4 and applying Theorem III.2, we get that

$$\left\| \int_0^1 F_{\mathbf{x}}(\mathbf{x}_n(t_k), \mathbf{u}_n(t_k)) b_{0,n}(t_k) dt - \int_0^1 F_{\mathbf{x}}(\mathbf{x}_n(t), \mathbf{u}_n(t)) b_{0,n}(t) dt \right\| \leq C_I W_{F_{\mathbf{x}} b_{0,n}} \left( \frac{1}{\sqrt{n}} \right) \quad (108)$$

where  $W_{F_{\mathbf{x}} b_{0,n}}(\cdot)$  is the modulus of continuity of the product  $F_{\mathbf{x}}(\mathbf{x}_n(t_k), \mathbf{u}_n(t_k)) b_{0,n}(t_k)$ . Then by using the continuity of both functions over the bounded domain and the properties of the modulus of continuity, we get that

$$\left\| \int_0^1 F_{\mathbf{x}}(\mathbf{x}_n(t_k), \mathbf{u}_n(t_k)) b_{0,n}(t_k) dt - \int_0^1 F_{\mathbf{x}}(\mathbf{x}_n(t), \mathbf{u}_n(t)) b_{0,n}(t) dt \right\| \leq C_I F_{\mathbf{x}, \max} \frac{1}{\sqrt{n}} + C_I W_{F_{\mathbf{x}}} \left( \frac{1}{\sqrt{n}} \right) \quad (109)$$

where  $F_{\mathbf{x}, \max}$  is the upper bound of  $F_{\mathbf{x}}(\mathbf{x}_n(t), \mathbf{u}_n(t))$ , which exists due to its continuity over the bounded domain, and  $W_{F_{\mathbf{x}}}(\cdot)$  is the modulus of continuity of  $F_{\mathbf{x}}$ . Furthermore, we have

$$\begin{aligned} & \left\| \int_0^1 F_{\mathbf{x}}(\mathbf{x}_n(t), \mathbf{u}_n(t)) b_{0,n}(t) dt - \int_0^1 F_{\mathbf{x}}(\mathbf{x}(t), \mathbf{u}(t)) b_{0,n}(t) dt \right\| \\ & \leq \int_0^1 \|F_{\mathbf{x}}(\mathbf{x}_n(t), \mathbf{u}_n(t)) - F_{\mathbf{x}}(\mathbf{x}(t), \mathbf{u}(t))\| \|b_{0,n}(t)\| dt \leq L_{F_{\mathbf{x}}} (\delta_{\mathbf{x}}^n + \delta_{\mathbf{u}}^n) \end{aligned} \quad (110)$$

where  $L_{F_{\mathbf{x}}}$  is the sum Lipschitz constant of  $F_{\mathbf{x}}$  with respect to  $\mathbf{x}$  and  $\mathbf{u}$ , and  $\|b_{0,n}(t)\| \leq 1$  for any  $t \in [0, 1]$ . Hence, we obtained that

$$\left\| \int_0^1 F_{\mathbf{x}}(\mathbf{x}_n(t_k), \mathbf{u}_n(t_k)) b_{0,n}(t_k) dt - \int_0^1 F_{\mathbf{x}}(\mathbf{x}(t), \mathbf{u}(t)) b_{0,n}(t) dt \right\| \leq \bar{C}_1 \left( \delta_{\mathbf{x}}^n + \delta_{\mathbf{u}}^n + \frac{1}{\sqrt{n}} \right) \quad (111)$$

where  $\bar{C}_1$  is a positive constant independent of  $n$ . Using similar arguments, we can show that

$$\left\| w \sum_{k=0}^{n_t} \bar{\lambda}_n^T(t_k) \dot{b}_{0,n}(t_k) - \int_0^1 \lambda^T(t) \dot{b}_{0,n}(t) dt \right\| \leq \bar{C}_2 \left( \delta_\lambda^n + \frac{1}{\sqrt{n}} \right) \mathbf{1} \quad (112)$$

$$\begin{aligned} & \left\| w \sum_{k=0}^{n_t} \bar{\lambda}_n^T(t_k) \mathbf{f}_x(\mathbf{x}_n(t_k), \mathbf{u}_n(t_k)) b_{0,n}(t_k) - \int_0^1 \lambda^T(t) \mathbf{f}_x(\mathbf{x}(t), \mathbf{u}(t)) b_{0,n}(t) dt \right\| \\ & \leq \bar{C}_3 \left( \delta_x^n + \delta_u^n + \delta_\lambda^n + \frac{1}{\sqrt{n}} \right) \mathbf{1} \end{aligned} \quad (113)$$

$$\begin{aligned} & \left\| w \sum_{k=0}^{n_t} \bar{\mu}_n^T(t_k) \mathbf{h}_x(\mathbf{x}_n(t_k), \mathbf{u}_n(t_k)) b_{0,n}(t_k) - \int_0^1 \mu^T(t) \mathbf{h}_x(\mathbf{x}(t), \mathbf{u}(t)) b_{0,n}(t) dt \right\| \\ & \leq \bar{C}_4 \left( \delta_x^n + \delta_u^n + \delta_\mu^n + \frac{1}{\sqrt{n}} \right) \mathbf{1} \end{aligned} \quad (114)$$

where  $\bar{C}_2$ ,  $\bar{C}_3$ , and  $\bar{C}_4$  are positive constants independent of  $n$ . Similarly, we can obtain that

$$\|E_{\mathbf{x}(0)}(\mathbf{x}_n(0), \mathbf{x}_n(1)) - E_{\mathbf{x}(0)}(\mathbf{x}(0), \mathbf{x}(1))\| \leq \bar{C}_5 \delta_x^n, \quad (115)$$

$$\|\bar{\mathbf{v}}^T \mathbf{e}_{\mathbf{x}(0)}(\mathbf{x}_n(0), \mathbf{x}_n(1)) - \bar{\mathbf{v}}^T \mathbf{e}_{\mathbf{x}(0)}(\mathbf{x}(0), \mathbf{x}(1))\| \leq \bar{C}_6 \delta_x^n. \quad (116)$$

where  $\bar{C}_5$  and  $\bar{C}_6$  are positive constants independent of  $n$ . Using these relations, we can write the following inequality

$$\begin{aligned} & \left\| \frac{\partial \mathcal{L}_n}{\partial \bar{\mathbf{c}}_{x,0}} \right\| \leq \left\| E_{\mathbf{x}(0)}(\mathbf{x}(0), \mathbf{x}(1)) + \int_0^1 F_x(\mathbf{x}(t), \mathbf{u}(t)) b_{0,n}(t) dt + \bar{\mathbf{v}}^T \mathbf{e}_{\mathbf{x}(0)}(\mathbf{x}(0), \mathbf{x}(1)) \right. \\ & - \int_0^1 \lambda^T(t) \dot{b}_{0,n}(t) dt + \int_0^1 \lambda^T(t) \mathbf{f}_x(\mathbf{x}(t), \mathbf{u}(t)) b_{0,n}(t) dt \\ & \left. + \int_0^1 \mu^T(t) \mathbf{h}_x(\mathbf{x}(t), \mathbf{u}(t)) b_{0,n}(t) dt \right\| + \bar{C} \max \left\{ \delta_x^n, \delta_u^n, \delta_\lambda^n, \delta_\mu^n, \frac{1}{\sqrt{n}} \right\} \end{aligned} \quad (117)$$

where  $\bar{C} > 4 \max_{i=1, \dots, 6} \{\bar{C}_i\}$ . We apply integration by parts to obtain:

$$\begin{aligned} \int_0^1 \lambda^T(t) \dot{b}_{0,n}(t) dt &= - \int_0^1 \dot{\lambda}^T(t) b_{0,n}(t) dt + \left[ \lambda^T(t) b_{0,n}(t) \right]_0^1 \\ &= - \int_0^1 \dot{\lambda}^T(t) b_{0,n}(t) dt - \lambda^T(0) \end{aligned} \quad (118)$$

where  $b_{0,n}(0) = 1$  and  $b_{0,n}(1) = 0$ . We get that

$$\begin{aligned}
& \left\| \frac{\partial \mathcal{L}_n}{\partial \bar{\mathbf{c}}_{x,0}} \right\| \leq \left\| E_{\mathbf{x}(0)}(\mathbf{x}(0), \mathbf{x}(1)) + \boldsymbol{\lambda}^T(0) + \bar{\mathbf{v}}^T \mathbf{e}_{\mathbf{x}(0)}(\mathbf{x}(0), \mathbf{x}(1)) \right\| \\
& + \left\| \int_0^1 \left( F_{\mathbf{x}}(\mathbf{x}(t), \mathbf{u}(t)) + \dot{\boldsymbol{\lambda}}^T(t) + \boldsymbol{\lambda}^T(t) \mathbf{f}_{\mathbf{x}}(\mathbf{x}(t), \mathbf{u}(t)) + \boldsymbol{\mu}^T(t) \mathbf{h}_{\mathbf{x}}(\mathbf{x}(t), \mathbf{u}(t)) \right) b_{0,n}(t) dt \right\| \\
& + \bar{C} \max \left\{ \delta_{\boldsymbol{\mu}}^n, \delta_{\mathbf{x}}^n, \delta_{\mathbf{u}}^n, \frac{1}{\sqrt{n}} \right\} \tag{119}
\end{aligned}$$

The first term is nulled by applying Eq. (62) and the second term using (61). Thus, this completes the proof for the first case of Eq. (69). By using identical arguments, we can also prove the other cases.

Similarly, we prove the stationarity conditions in (69) for the Fourier part of the approximation.

Consider:

$$\begin{aligned}
& \left\| \frac{\partial \mathcal{L}_n}{\partial \bar{\mathbf{a}}_{x,1}} \right\| = \left\| E_{\mathbf{x}(0)}(\mathbf{x}_n(0), \mathbf{x}_n(1)) + E_{\mathbf{x}(1)}(\mathbf{x}_n(0), \mathbf{x}_n(1)) + w \sum_{k=0}^{n_t} F_{\mathbf{x}}(\mathbf{x}_n(t_k), \mathbf{u}_n(t_k)) c_1(t_k) \right. \\
& + \sum_{k=0}^{n_t} \boldsymbol{\lambda}_n^T(t_k) \left( \mathbf{f}_{\mathbf{x}}(\mathbf{x}_n(t_k), \mathbf{u}_n(t_k)) c_1(t_k) - \dot{c}_1(t_k) \right) + \sum_{k=0}^{n_t} \boldsymbol{\mu}_n^T(t_k) \mathbf{h}_{\mathbf{x}}(\mathbf{x}_n(t_k), \mathbf{u}_n(t_k)) c_1(t_k) \\
& \left. + \bar{\mathbf{v}}^T \mathbf{e}_{\mathbf{x}(0)}(\mathbf{x}_n(0), \mathbf{x}_n(1)) + \bar{\mathbf{v}}^T \mathbf{e}_{\mathbf{x}(1)}(\mathbf{x}_n(0), \mathbf{x}_n(1)) \right\| \\
& = \left\| E_{\mathbf{x}(0)}(\mathbf{x}_n(0), \mathbf{x}_n(1)) + E_{\mathbf{x}(1)}(\mathbf{x}_n(0), \mathbf{x}_n(1)) + w \sum_{k=0}^{n_t} F_{\mathbf{x}}(\mathbf{x}_n(t_k), \mathbf{u}_n(t_k)) c_1(t_k) \right. \\
& + w \sum_{k=0}^{n_t} \bar{\boldsymbol{\lambda}}_n^T(t_k) \left( \mathbf{f}_{\mathbf{x}}(\mathbf{x}_n(t_k), \mathbf{u}_n(t_k)) c_1(t_k) - \dot{c}_1(t_k) \right) + w \sum_{k=0}^{n_t} \bar{\boldsymbol{\mu}}_n^T(t_k) \mathbf{h}_{\mathbf{x}}(\mathbf{x}_n(t_k), \mathbf{u}_n(t_k)) c_1(t_k) \\
& \left. + \bar{\mathbf{v}}^T \mathbf{e}_{\mathbf{x}(0)}(\mathbf{x}_n(0), \mathbf{x}_n(1)) + \bar{\mathbf{v}}^T \mathbf{e}_{\mathbf{x}(1)}(\mathbf{x}_n(0), \mathbf{x}_n(1)) \right\| \tag{120}
\end{aligned}$$

where  $c_j(t_k) \triangleq \cos(2\pi j t_k)$  and  $\dot{c}_j(t_k)$  is its time derivative, and in the second equality we substitute  $\boldsymbol{\lambda}_n^T(t_k) = w \bar{\boldsymbol{\lambda}}_n^T(t_k)$  and  $\boldsymbol{\mu}_n^T(t_k) = w \bar{\boldsymbol{\mu}}_n^T(t_k)$ . Using similar arguments to those used to prove

Eqs. (111)–(114), we get that

$$\left\| w \sum_{k=0}^{n_t} F_{\mathbf{x}}(\mathbf{x}_n(t_k), \mathbf{u}_n(t_k))c_1(t_k) - \int_0^1 F_{\mathbf{x}}(\mathbf{x}(t), \mathbf{u}(t))c_1(t)dt \right\| \leq \bar{C}_7 \left( \delta_{\mathbf{x}}^n + \delta_{\mathbf{u}}^n + \frac{1}{\sqrt{n}} \right) \quad (121)$$

$$\left\| w \sum_{k=0}^{n_t} \bar{\lambda}_n^T(t_k) \dot{c}_1(t_k) - \int_0^1 \lambda^T(t) \dot{c}_1(t)dt \right\| \leq \bar{C}_8 \left( \delta_{\lambda}^n + \frac{1}{\sqrt{n}} \right) \mathbf{1} \quad (122)$$

$$\begin{aligned} & \left\| w \sum_{k=0}^{n_t} \bar{\lambda}_n^T(t_k) \mathbf{f}_{\mathbf{x}}(\mathbf{x}_n(t_k), \mathbf{u}_n(t_k))c_1(t_k) - \int_0^1 \lambda^T(t) \mathbf{f}_{\mathbf{x}}(\mathbf{x}(t), \mathbf{u}(t))c_1(t)dt \right\| \\ & \leq \bar{C}_9 \left( \delta_{\mathbf{x}}^n + \delta_{\mathbf{u}}^n + \delta_{\lambda}^n + \frac{1}{\sqrt{n}} \right) \mathbf{1} \end{aligned} \quad (123)$$

$$\begin{aligned} & \left\| w \sum_{k=0}^{n_t} \bar{\mu}_n^T(t_k) \mathbf{h}_{\mathbf{x}}(\mathbf{x}_n(t_k), \mathbf{u}_n(t_k))c_1(t_k) - \int_0^1 \mu^T(t) \mathbf{h}_{\mathbf{x}}(\mathbf{x}(t), \mathbf{u}(t))c_1(t)dt \right\| \\ & \leq \bar{C}_{10} \left( \delta_{\mathbf{x}}^n + \delta_{\mathbf{u}}^n + \delta_{\mu}^n + \frac{1}{\sqrt{n}} \right) \mathbf{1} \end{aligned} \quad (124)$$

where  $\bar{C}_7$ ,  $\bar{C}_8$ ,  $\bar{C}_9$ , and  $\bar{C}_{10}$  are positive constants independent of  $n$ . We can also obtain that

$$\left\| E_{\mathbf{x}(1)}(\mathbf{x}_n(0), \mathbf{x}_n(1)) - E_{\mathbf{x}(1)}(\mathbf{x}(0), \mathbf{x}(1)) \right\| \leq \bar{C}_{11} \delta_{\mathbf{x}}^n, \quad (125)$$

$$\left\| \bar{\mathbf{v}}^T \mathbf{e}_{\mathbf{x}(1)}(\mathbf{x}_n(0), \mathbf{x}_n(1)) - \bar{\mathbf{v}}^T \mathbf{e}_{\mathbf{x}(1)}(\mathbf{x}(0), \mathbf{x}(1)) \right\| \leq \bar{C}_{12} \delta_{\mathbf{x}}^n. \quad (126)$$

where  $\bar{C}_{11}$  and  $\bar{C}_{12}$  are positive constants independent of  $n$ . Using these relations, we can write the following inequality

$$\begin{aligned} & \left\| \frac{\partial \mathcal{L}_n}{\partial \mathbf{a}_{x,1}} \right\| \leq \left\| E_{\mathbf{x}(0)}(\mathbf{x}(0), \mathbf{x}(1)) + \int_0^1 F_{\mathbf{x}}(\mathbf{x}(t), \mathbf{u}(t))c_1(t)dt + \bar{\mathbf{v}}^T \mathbf{e}_{\mathbf{x}(0)}(\mathbf{x}(0), \mathbf{x}(1)) \right. \\ & + E_{\mathbf{x}(1)}(\mathbf{x}(0), \mathbf{x}(1)) + \bar{\mathbf{v}}^T \mathbf{e}_{\mathbf{x}(1)}(\mathbf{x}(0), \mathbf{x}(1)) \\ & - \int_0^1 \lambda^T(t) \dot{c}_1(t)dt + \int_0^1 \lambda^T(t) \mathbf{f}_{\mathbf{x}}(\mathbf{x}(t), \mathbf{u}(t))c_1(t)dt \\ & \left. + \int_0^1 \mu^T(t) \mathbf{h}_{\mathbf{x}}(\mathbf{x}(t), \mathbf{u}(t))b_{0,n}(t)dt \right\| + \bar{C} \max \left\{ \delta_{\mathbf{x}}^n, \delta_{\mathbf{u}}^n, \delta_{\lambda}^n, \delta_{\mu}^n, \frac{1}{\sqrt{n}} \right\} \end{aligned} \quad (127)$$

where  $\bar{C} > 4 \max_{i=7,\dots,12} \{\bar{C}_i\}$ . We apply integration by parts to obtain:

$$\begin{aligned} \int_0^1 \lambda^T(t) \dot{c}_1(t) dt &= - \int_0^1 \dot{\lambda}^T(t) c_1(t) dt + \left[ \lambda^T(t) c_1(t) \right]_0^1 \\ &= - \int_0^1 \dot{\lambda}^T(t) c_1(t) dt + \lambda^T(1) - \lambda^T(0) \end{aligned} \quad (128)$$

where  $c_1(0) = c_1(1) = 1$ . We get that

$$\begin{aligned} \left\| \frac{\partial \mathcal{L}_n}{\partial \mathbf{a}_{x,1}} \right\| &\leq \left\| E_{\mathbf{x}(0)}(\mathbf{x}(0), \mathbf{x}(1)) + \lambda^T(0) + \bar{\mathbf{v}}^T \mathbf{e}_{\mathbf{x}(0)}(\mathbf{x}(0), \mathbf{x}(1)) \right\| \\ &+ \left\| E_{\mathbf{x}(1)}(\mathbf{x}(0), \mathbf{x}(1)) - \lambda^T(1) + \bar{\mathbf{v}}^T \mathbf{e}_{\mathbf{x}(1)}(\mathbf{x}(0), \mathbf{x}(1)) \right\| \\ &+ \left\| \int_0^1 \left( F_{\mathbf{x}}(\mathbf{x}(t), \mathbf{u}(t)) + \dot{\lambda}^T(t) + \lambda^T(t) \mathbf{f}_{\mathbf{x}}(\mathbf{x}(t), \mathbf{u}(t)) + \boldsymbol{\mu}^T(t) \mathbf{h}_{\mathbf{x}}(\mathbf{x}(t), \mathbf{u}(t)) \right) c_1(t) dt \right\| \\ &+ \bar{C} \max \left\{ \delta_{\boldsymbol{\mu}}^n, \delta_{\mathbf{x}}^n, \delta_{\mathbf{u}}^n, \frac{1}{\sqrt{n}} \right\} \end{aligned} \quad (129)$$

The first two terms are nulled by applying Eq. (62) and (63), and the last term is nulled using (61). Thus, this completes the proof for the first Fourier coefficient in Eq. (69). By using identical arguments, we can also prove the other cases.

The first closure condition (70) satisfies

$$\begin{aligned} &\left\| \frac{\lambda_n^T(0)}{w} + \bar{\mathbf{v}}^T \mathbf{e}_{\mathbf{x}(0)}(\mathbf{x}_n(0), \mathbf{x}_n(1)) + E_{\mathbf{x}(0)}(\mathbf{x}_n(0), \mathbf{x}_n(1)) \right\| \\ &= \left\| \bar{\lambda}_n^T(0) + \bar{\mathbf{v}}^T \mathbf{e}_{\mathbf{x}(0)}(\mathbf{x}_n(0), \mathbf{x}_n(1)) + E_{\mathbf{x}(0)}(\mathbf{x}_n(0), \mathbf{x}_n(1)) \right\| \\ &\leq \left\| \lambda^T(0) + \mathbf{v}^T \mathbf{e}_{\mathbf{x}(0)}(\mathbf{x}(0), \mathbf{x}(1)) + E_{\mathbf{x}(0)}(\mathbf{x}(0), \mathbf{x}(1)) \right\| + \delta_{\lambda}^n + (\bar{C}_5 + \bar{C}_6) \delta_{\mathbf{x}}^n \end{aligned} \quad (130)$$

where the first term after the inequality is nulled by applying Eq. (62), and  $C_D > 2 \max\{1, (\bar{C}_5 + \bar{C}_6)\}$ .

Using the same arguments, we can show that the other closure condition in (71) also satisfies its inequality constraint.  $\square$

## D. Proof of Th. V.2

*Proof.* We show that  $\mathbf{x}_n(t_k)$ ,  $\mathbf{u}_n(t_k)$ ,  $\lambda_n(t_k)$ ,  $\boldsymbol{\mu}_n(t_k)$ , and  $\bar{\mathbf{v}}$  satisfy the conditions in Eqs. (46)–(48) and the condition of the dual variables in (60)–(64). Th. IV.2 shows the satisfaction of the conditions of the primal variables. Similarly to the first step of the proof of Th. IV.2, we show that Eq. (60) holds by contradiction. We assume that  $\mathbf{x}^\infty(t)$ ,  $\mathbf{u}^\infty(t)$  and,  $\boldsymbol{\mu}^\infty(t)$  do not satisfy (60). Thus, there exists  $t' \in [0, 1]$ , such that

$$\|(\bar{\boldsymbol{\mu}}^\infty)^T(t')\mathbf{h}(\mathbf{x}^\infty(t'), \mathbf{u}^\infty(t'))\| > 0. \quad (131)$$

Because  $\{t_k\}_{k=0}^\infty$  is dense in  $[0, 1]$ , there exists a subsequence with indices  $\{k_n\}_{n=0}^\infty$  such that

$$\lim_{n \rightarrow \infty} t_{k_n} = t', \quad (132)$$

hence

$$\lim_{n \rightarrow \infty} \|\bar{\boldsymbol{\mu}}^\infty(t') - \bar{\boldsymbol{\mu}}^\infty(t_{k_n})\| = 0, \quad (133)$$

$$\lim_{n \rightarrow \infty} \|\mathbf{x}^\infty(t') - \mathbf{x}^\infty(t_{k_n})\| = 0, \quad (134)$$

$$\lim_{n \rightarrow \infty} \|\mathbf{u}^\infty(t') - \mathbf{u}^\infty(t_{k_n})\| = 0. \quad (135)$$

Next, we add and subtract  $\bar{\boldsymbol{\mu}}_n^T(t_{k_n})(\mathbf{h}(\mathbf{x}_n(t'), \mathbf{u}_n(t')) - \mathbf{h}(\mathbf{x}_n(t_{k_n}), \mathbf{u}_n(t_{k_n})))$ , then use the triangle inequality to obtain:

$$\begin{aligned} & \|(\bar{\boldsymbol{\mu}}^\infty)^T(t')\mathbf{h}(\mathbf{x}^\infty(t'), \mathbf{u}^\infty(t'))\| \leq \lim_{n \rightarrow \infty} \|(\bar{\boldsymbol{\mu}}_n^T(t') - \bar{\boldsymbol{\mu}}_n^T(t_{k_n}))\mathbf{h}(\mathbf{x}_n(t'), \mathbf{u}_n(t'))\| \\ & + \lim_{n \rightarrow \infty} \|\bar{\boldsymbol{\mu}}_n^T(t_{k_n})(\mathbf{h}(\mathbf{x}_n(t'), \mathbf{u}_n(t')) - \mathbf{h}(\mathbf{x}_n(t_{k_n}), \mathbf{u}_n(t_{k_n})))\| \\ & + \lim_{n \rightarrow \infty} \|\bar{\boldsymbol{\mu}}_n^T(t_{k_n})\mathbf{h}(\mathbf{x}_n(t_{k_n}), \mathbf{u}_n(t_{k_n}))\| \\ & = \lim_{n \rightarrow \infty} \frac{1}{W} \|\boldsymbol{\mu}_n^T(t_{k_n})\mathbf{h}(\mathbf{x}_n(t_{k_n}), \mathbf{u}_n(t_{k_n}))\| = 0, \end{aligned} \quad (136)$$

where we used Eq. (68). This contradicts Eq. (131). Using similar arguments, we can show that  $\bar{\boldsymbol{\mu}}^\infty \geq 0$ , thus proving that  $\mathbf{x}^\infty(t)$ ,  $\mathbf{u}^\infty(t)$ , and  $\bar{\boldsymbol{\mu}}^\infty$  satisfy Eq. (60).

Then, we notice that because  $\mathbf{x}^\infty(t)$ ,  $\mathbf{u}^\infty(t)$ ,  $\bar{\lambda}^\infty(t)$ ,  $\bar{\mu}^\infty(t)$ , and  $\bar{\mathbf{v}}^\infty$  also satisfy Eqs.(69)–(71), then the following relations hold:

$$\left\| \bar{\lambda}^\infty(0) + (\bar{\mathbf{v}}^\infty)^T \mathbf{e}_{\mathbf{x}(0)}(\mathbf{x}^\infty(0), \mathbf{x}^\infty(1)) + E_{\mathbf{x}(0)}(\mathbf{x}^\infty(0), \mathbf{x}^\infty(1)) \right\| = 0,$$

$$\left\| \bar{\lambda}^\infty(1) - (\bar{\mathbf{v}}^\infty)^T \mathbf{e}_{\mathbf{x}(1)}(\mathbf{x}^\infty(0), \mathbf{x}^\infty(1)) - E_{\mathbf{x}(1)}(\mathbf{x}^\infty(0), \mathbf{x}^\infty(1)) \right\| = 0,$$

$$\left\| \int_0^1 \left[ (\dot{\bar{\lambda}}^\infty)^T(t) + F_{\mathbf{x}}(\mathbf{x}^\infty(t), \mathbf{u}^\infty(t)) + (\bar{\lambda}^\infty)^T(t) \mathbf{f}_{\mathbf{x}}(\mathbf{x}^\infty(t), \mathbf{u}^\infty(t)) + (\bar{\mu}^\infty)^T(t) \mathbf{h}_{\mathbf{x}}(\mathbf{x}^\infty(t), \mathbf{u}^\infty(t)) \right] b_{k,n}(t) dt \right\| = 0,$$

$$\left\| \int_0^1 \left[ F_{\mathbf{u}}(\mathbf{x}^\infty(t), \mathbf{u}^\infty(t)) + (\bar{\lambda}^\infty)^T(t) \mathbf{f}_{\mathbf{u}}(\mathbf{x}^\infty(t), \mathbf{u}^\infty(t)) + (\bar{\mu}^\infty)^T(t) \mathbf{h}_{\mathbf{u}}(\mathbf{x}^\infty(t), \mathbf{u}^\infty(t)) \right] b_{k,n}(t) dt \right\| = 0,$$

for any  $k = 0, \dots, n_B$ . Similar results for the last two relations can be obtained with  $c_k(t)$  instead of  $b_{k,n}(t)$ . Because  $\{b_{k,n}(t)\}_{k=0}^{n_B}$  is a linearly independent basis set (and  $\{c_k(t)\}_{k=0}^{n_F}$  is a linearly independent set), thus

$$\left\| (\dot{\bar{\lambda}}^\infty)^T(t) + F_{\mathbf{x}}(\mathbf{x}^\infty(t), \mathbf{u}^\infty(t)) + (\bar{\lambda}^\infty)^T(t) \mathbf{f}_{\mathbf{x}}(\mathbf{x}^\infty(t), \mathbf{u}^\infty(t)) + (\bar{\mu}^\infty)^T(t) \mathbf{h}_{\mathbf{x}}(\mathbf{x}^\infty(t), \mathbf{u}^\infty(t)) \right\| = 0,$$

$$\left\| F_{\mathbf{u}}(\mathbf{x}^\infty(t), \mathbf{u}^\infty(t)) + (\bar{\lambda}^\infty)^T(t) \mathbf{f}_{\mathbf{u}}(\mathbf{x}^\infty(t), \mathbf{u}^\infty(t)) + (\bar{\mu}^\infty)^T(t) \mathbf{h}_{\mathbf{u}}(\mathbf{x}^\infty(t), \mathbf{u}^\infty(t)) \right\| = 0,$$

for any  $t \in [0, 1]$ .

Therefore, we have shown that  $\mathbf{x}^\infty(t)$ ,  $\mathbf{u}^\infty(t)$ ,  $\bar{\lambda}^\infty(t)$ ,  $\bar{\mu}^\infty(t)$ , and  $\bar{\mathbf{v}}^\infty$  satisfy Eqs.(61)–(64).  $\square$

## References

- [1] Betts, J. T., *Practical Methods for Optimal Control and Estimation Using Nonlinear Programming: Second Edition*, SIAM, 2010, Chap. 4.
- [2] Polak, E., *Optimization: Algorithms and Consistent Approximations*, Springer, New York, NY, 1997, Applied Mathematical Sciences, Vol. 124, Chap. 4.
- [3] Schwartz, A., and Polak, E., “Consistent Approximations for Optimal Control Problems Based

- on Runge–Kutta Integration,” *SIAM J. Control Optim.*, Vol. 34, No. 4, 1996, pp. 1235–1269. <https://doi.org/10.1137/S0363012994267352>.
- [4] Ross, I. M., and Karpenko, M., “A review of pseudospectral optimal control: From theory to flight,” *Annual Reviews in Control*, Vol. 36, No. 2, 2012, pp. 182–197. <https://doi.org/10.1016/j.arcontrol.2012.09.002>.
- [5] Cichella, V., Kaminer, I., Walton, C., Hovakimyan, N., and Pascoal, A. M., “Optimal Multivehicle Motion Planning Using Bernstein Approximants,” *IEEE Transactions on Automatic Control*, Vol. 66, No. 4, 2021, pp. 1453–1467. <https://doi.org/10.1109/TAC.2020.2999329>.
- [6] Kirk, D. E., *Optimal Control Theory: An Introduction*, Courier Corporation, 2004, Chap. 5.
- [7] Hager, W. W., “Runge-Kutta methods in optimal control and the transformed adjoint system,” *Numer. Math.*, Vol. 87, No. 2, 2000, pp. 247–282. <https://doi.org/10.1007/s002110000178>.
- [8] Gong, Q., Ross, I. M., Kang, W., and Fahroo, F., “Connections between the covector mapping theorem and convergence of pseudospectral methods for optimal control,” *Comput Optim Appl*, Vol. 41, No. 3, 2008, pp. 307–335. <https://doi.org/10.1007/s10589-007-9102-4>.
- [9] Garg, D., Patterson, M., Hager, W. W., Rao, A. V., Benson, D. A., and Huntington, G. T., “A unified framework for the numerical solution of optimal control problems using pseudospectral methods,” *Automatica*, Vol. 46, No. 11, 2010, pp. 1843–1851. <https://doi.org/10.1016/j.automatica.2010.06.048>.
- [10] Cichella, V., Kaminer, I., Walton, C., Hovakimyan, N., and Pascoal, A., “Consistency of Approximation of Bernstein Polynomial-Based Direct Methods for Optimal Control,” *Machines*, Vol. 10, No. 12, 2022, p. 1132. <https://doi.org/10.3390/machines10121132>.
- [11] Kielas-Jensen, C., Cichella, V., Berry, T., Kaminer, I., Walton, C., and Pascoal, A., “Bernstein Polynomial-Based Method for Solving Optimal Trajectory Generation Problems,” *Sensors*, Vol. 22, No. 5, 2022, p. 1869. <https://doi.org/10.3390/s22051869>.
- [12] Strano, B., Furci, M., and Marconi, L., “Kinodynamic optimal trajectories generation in cluttered environments using Bernstein polynomials,” *Mechatronics*, Vol. 92, 2023, p. 102969. <https://doi.org/10.1016/j.mechatronics.2023.102969>.

- [13] Ross, I. M., Proulx, R. J., and Borges, C. F., “A universal Birkhoff pseudospectral method for solving boundary value problems,” *Applied Mathematics and Computation*, Vol. 454, 2023, p. 128101. <https://doi.org/10.1016/j.amc.2023.128101>.
- [14] Gong, Q., Ross, I. M., and Fahroo, F., “Spectral and Pseudospectral Optimal Control Over Arbitrary Grids,” *J. Optim. Theory Appl.*, Vol. 169, No. 3, 2016, pp. 759–783. <https://doi.org/10.1007/s10957-016-0909-y>.
- [15] Hammel, S. E., Liu, P. T., Hilliard, E. J., and Gong, K. F., “Optimal observer motion for localization with bearing measurements,” *Computers & Mathematics with Applications*, Vol. 18, No. 1, 1989, pp. 171–180. [https://doi.org/10.1016/0898-1221\(89\)90134-X](https://doi.org/10.1016/0898-1221(89)90134-X).
- [16] Oshman, Y., and Davidson, P., “Optimization of observer trajectories for bearings-only target localization,” *IEEE Transactions on Aerospace and Electronic Systems*, Vol. 35, No. 3, 1999, pp. 892–902. <https://doi.org/10.1109/7.784059>.
- [17] Ponda, S., Kolacinski, R., and Frazzoli, E., “Trajectory Optimization for Target Localization Using Small Unmanned Aerial Vehicles,” *AIAA Guidance, Navigation, and Control Conference*, AIAA, 2009, p. 6015. <https://doi.org/https://doi.org/10.2514/6.2009-6015>.
- [18] Frey, G. R., Petersen, C. D., Leve, F. A., Kolmanovsky, I. V., and Girard, A. R., “Constrained Spacecraft Relative Motion Planning Exploiting Periodic Natural Motion Trajectories and Invariance,” *Journal of Guidance, Control, and Dynamics*, Vol. 40, No. 12, 2017, pp. 3100–3115. <https://doi.org/10.2514/1.G002914>.
- [19] Taheri, E., Kolmanovsky, I., and Atkins, E., “Shaping low-thrust trajectories with thrust-handling feature,” *Advances in Space Research*, Vol. 61, No. 3, 2018, pp. 879–890. <https://doi.org/10.1016/j.asr.2017.11.006>.
- [20] Mudrik, L., Kragelund, S., and Kaminer, I., “Optimal Motion Planning Using Mixed Bernstein-Fourier Approximants,” *2025 American Control Conference (ACC)*, AIAA, Denver, CO, 2025.
- [21] Floater, M. S., “On the convergence of derivatives of Bernstein approximation,” *Journal of Approximation Theory*, Vol. 134, No. 1, 2005, pp. 130–135. <https://doi.org/10.1016/j.jat.2004.02.009>.

- [22] Jackson, D., *The Theory of Approximation*, American Mathematical Soc., 1930, Chap. 1.
- [23] Boyd, S., and Vandenberghe, L., *Introduction to Applied Linear Algebra: Vectors, Matrices, and Least Squares*, Cambridge University Press, 2018, Chap. 15.
- [24] Ross, I. M., Gong, Q., and Sekhavat, P., “Low-Thrust, High-Accuracy Trajectory Optimization,” *Journal of Guidance, Control, and Dynamics*, Vol. 30, No. 4, 2007, pp. 921–933. <https://doi.org/10.2514/1.23181>.
- [25] Hartl, R. F., Sethi, S. P., and Vickson, R. G., “A Survey of the Maximum Principles for Optimal Control Problems with State Constraints,” *SIAM Rev.*, Vol. 37, No. 2, 1995, pp. 181–218. <https://doi.org/10.1137/1037043>.
- [26] Fahroo, F., and Ross, I. M., “Costate Estimation by a Legendre Pseudospectral Method,” *Journal of Guidance, Control, and Dynamics*, Vol. 24, No. 2, 2001, pp. 270–277. <https://doi.org/10.2514/2.4709>.
- [27] Hung, N. T., Crasta, N., Moreno-Salinas, D., Pascoal, A. M., and Johansen, T. A., “Range-based target localization and pursuit with autonomous vehicles: An approach using posterior CRLB and model predictive control,” *Robotics and Autonomous Systems*, Vol. 132, 2020, p. 103608. <https://doi.org/10.1016/j.robot.2020.103608>.
- [28] Gong, Q., Ross, I. M., and Fahroo, F., “Costate Computation by a Chebyshev Pseudospectral Method,” *Journal of Guidance, Control, and Dynamics*, Vol. 33, No. 2, 2010, pp. 623–628. <https://doi.org/10.2514/1.45154>.